의학박사 학위논문

Comprehensive analysis of expression of immune checkpoint receptors and human leukocyte antigen class I in stage II and III gastric cancer

2기 및 3기 위암에서 면역 관문 수용체와 제1급 인간 백혈구 항원 발현에 대한 통합적 분석

February 2022

서울대학교 대학원
의학과 병리학전공
박 유 준

Comprehensive analysis of expression of immune checkpoint receptors and human leukocyte antigen class I in stage II and III gastric cancer

October 2021

Graduate School of Medicine
Seoul National University
Pathology Major

Yu Jun Park

Confirming the Ph.D. Dissertation written by
Yu Jun Park
January 2022

Chair	_____(Seal)
Vice Chair	_____(Seal)
Examiner	_____(Seal)
Examiner	_____(Seal)
Examiner	_____(Seal)

2기 및 3기 위암에서 면역 관문 수용체와 제1급 인간 백혈구 항원 발현에 대한 통합적 분석

지도교수 이 혜 승

이 논문을 의학박사 학위논문으로 제출함
2021년 10월

서울대학교 대학원
의학과 병리학전공
박 유 준

박유준의 의학박사 학위논문을 인준함
2022년 1월

위 원 장 _____(인)
부위원장 _____(인)
위 원 _____(인)
위 원 _____(인)
위 원 _____(인)

Abstract

Solid tumors elicit a tumor-associated immune response. Tumor cells have characteristics that can avoid tumor immune responses, such as loss of human leukocyte antigen (HLA) class I (HLA I) presentation on the tumor cell surface and increased immune checkpoint receptors (ICRs) expression in tumor-infiltrating immune cells (TIICs). HLA I molecules, composed of alpha (heavy) chain, including HLA-A, -B, or -C encoded by HLA genes, and beta-2-microglobulin (β2M), are membrane proteins on all nucleated cells that display peptide antigens for recognition by CD8+ cytotoxic T cells. The ICRs, such as programmed death receptor 1 (PD-1), lymphocyte activation gene-3 (LAG3), and T cell immunoglobulin and mucin domain 3 (TIM3) mediate immune tolerance and immune evasion of cancer cells, thus there have tried to employ immune checkpoint inhibitors for systemic therapy in various solid cancers. However, a comprehensive analysis of HLA I and ICRs expression in gastric cancer (GC) is lacking.

Here, I sought to determine the clinicopathological significance of HLA I molecule expression in cancer cells and PD-1, LAG3, and TIM3 expression in TIICs in GCs.

Immunohistochemistry (IHC) for HLA A/B/C, β2M, PD-1, TIM3, LAG3, PD-L1 and TIICs markers was performed in center (CT) and invasive margin (IM) of the tumor in 406 patients with stage II and III GC using tissue microarray. Among the IHC results, 395 cases for HLA I molecules and 385 cases for ICRs were suitable for analysis. Epstein-Barr virus (EBV) in situ hybridization, microsatellite stability (MSI) testing, E-cadherin, and p53 IHC were performed for molecular classification. Chromogenic multiplex

IHC (mIHC) for PD-1, TIM3, LAG3, CD8, CD3, FOXP3, CD68, and cytokeratin was performed in 58 of the total samples.

Negative expression of HLA A/B/C and β2M in cancer cells was observed in 258 (65.3%) and 235 (59.5%) of 395 stage II and III GCs, respectively. Negative HLA I expression was significantly associated with aggressive clinicopathologic features. Furthermore, negative expression of HLA A/B/C and β2M was inversely correlated with $CD8^+$ cytotoxic T cell infiltration, EBV+, and PD-L1+ expression (all $p < 0.001$). Intact HLA A/B/C and β2M expression showed a significant correlation with PD-1, TIM3 and LAG3-positive expression (all $p < 0.001$). Patients with HLA A/B/C-negative GC had worse overall survival (OS) ($p = 0.019$) and combined analysis with both HLA A/B/C and β2M expression status significantly predicted worse OS in univariate ($p = 0.004$) and multivariate survival analysis ($p = 0.016$).

PD-1, LAG3, and TIM3 expression in TIICs was observed in 91 (23.6%), 193 (50.1%), and 257 (66.8%) GCs by single IHC, respectively. The ICRs expression was associated with high TIICs density and EBV^+ and MSI-H molecular subtypes (all $p \leq 0.01$). TIM3 was more expressed in epithelial-mesenchymal transition type GC than PD-1 and LAG3. LAG3 expression in the invasive margin of the tumor was significantly associated with better prognosis in univariate ($p = 0.020$) and multivariate ($p = 0.026$) survival analyses. The expression of the different ICRs was significantly positively correlated.

Dual or triple ICR expression was more frequent in high PD-1 and TIM3 density groups than in low-density groups by mIHC (all $p \leq 0.05$). ICRs were mainly expressed in $CD3^+CD8^+$ and $CD3^+CD8^-$ T cells. ICR-expressing $CD3^+CD8^+$ T cells were more

distributed in the intratumoral area than in the stroma. Fifty-eight GCs were classified into three groups by clustering analysis based on the mIHC results, and the group with the highest ICR expression in TIICs, which included all EBV subtype cases, showed significantly better outcomes in progression-free survival ($p = 0.020$).

In this study, negative expression of HLA A/B/C and β2M in cancer cells was frequently observed in stage II and III GCs, particularly with the aggressive clinicopathologic features, and correlated with an unfavorable prognosis and host immune response status. However, PD-1, LAG3, and TIM3 expression in TIICs is positively correlated and dual or triple expression of ICRs is more common in cases with high ICRs' expression by single IHC. ICR expression was also associated with a better prognosis. This study provides key information for the application of effective immune checkpoint inhibitors against GC.

Keyword : Gastric cancer, Immune checkpoint receptor, Human leukocyte antigen class I, Immunochemistry, Tumor microenvironment
Student Number : 2018-37505

Table of Contents

List of Tables

List of Figures

Chapter 1. Introduction

1.1. Study Background

Gastric cancer (GC) is one of the most common human cancers worldwide and is the third leading cause of death [1]. In South Korea, GC is the leading cause of cancer deaths in both men and women [2]. The 5-year relative survival rate of patients with early GC is over 90%, but that of patients with stage II or III GC is approximately 55% [3]. Adjuvant therapy after D2 gastrectomy improves overall survival (OS) in patients with stage II and III GC, but more than 30% of those with stage III GC exhibit recurrence after surgery [4]. Therefore, with recent developments in targeted therapies for GC [5], molecular targeted therapies have become increasingly necessary based on the molecular understanding of GC, including cancer cell genetics and immune microenvironment.

Various solid tumors, including GC, induce tumor-associated immune responses [6]. However, tumor cells can be evaded from immune responses, by the mechanism such as decreased or loss expression of human leukocyte antigen (HLA) class I (HLA I) on the tumor cell surface and increased expression of immune checkpoint receptors (ICRs) in tumor-infiltrating immune cells (TIICs) [7]. HLA I molecules are found on all nucleated cell surfaces and are key molecules involved in the cell-mediated immune system driven by $CD8^+$ cytotoxic T cells [8]. In cancer patients, neoantigens are presented via HLA I molecules on the cancer cell surface, thereby initiating a cell-mediated immune response to recruit $CD8^+$ cytotoxic T cells around the cancer cells. HLA I molecules consist of alpha (heavy) chain including HLA-A, -B, or -C encoded by *HLA* genes and beta-2-microglobulin (β2M). HLA I expression on cancer cells has been reported to be heterogenous and often found to be reduced or lost in many cancers [8, 9]. Additionally, the loss of HLA I heavy chain and β2M has been suggested as an immune escape mechanism in certain cancers

[10, 11]. However, the clinical significance of decreased or lost HLA I expression has not been investigated in patients with GC.

Recent studies have examined the immune escape mechanism in cancers [12], and clinical trials of checkpoint inhibitor therapy, especially various programmed cell death protein 1 (PD-1) inhibitors have shown beneficial outcomes in patients with solid tumors, including GC [13]. Based on the results of the KEYNOTE 059 trial, pembrolizumab was approved by the FDA in 2017 for pre-treated metastatic and programmed death-ligand 1 (PD-L1)-expressing GC patients [14, 15]. Although PD-L1 expression on the cancer cell surface, assessed by immunohistochemistry (IHC), was correlated with a therapeutic response [16, 17], predicting the therapeutic benefit and efficacy was not possible in all patients [18]. Therefore, identifying new biomarkers that can predict therapeutic effects in patients is currently under intense study [19]. Recent studies showed that inactivating mutations in β2M are associated with immunotherapy resistance [20] and suggested the importance of HLA I expression loss in predicting the therapeutic effect of immunotherapy [21, 22]. Therefore, the relationship between PD-L1 and HLA I expression must be verified to understand the immune microenvironment in GCs.

The PD-1/PD-L1 checkpoint plays an important role in host immune system evasion in various cancers [23]. PD-L1 expression in GC has been reported in previous studies, and it has been observed in the membranes of GC cells and in the cytoplasm with or without membrane expression of various immune cells. In particular, PD-L1 expression is significantly positively correlated with Epstein-Barr virus (EBV)-associated GCs and microsatellite instability (MSI)-high (MSI-H) GCs [24], which are characterized by immune cell-rich stroma.

In addition to PD-1, several ICRs control T cell-mediated cytotoxic reactions, including lymphocyte activation gene-3 (LAG3) and T cell immunoglobulin and mucin domain 3 (TIM3). LAG3 is a potential cancer immunotherapeutic target because it

regulates T cell activity. It is structurally similar to CD4 [25], binds to HLA class II molecules expressed by antigen-presenting cells or aberrantly by cancer cells, and mediates an intrinsic negative inhibitory signal, resulting in immune tolerance and immune evasion of cancer cells [26]. LAG3 is expressed on activated human T and natural killer (NK) cells [27]. TIM3 is a member of the TIM gene family and plays a role in suppressing T cell responses and inducing peripheral immune tolerance [28]. It is predominantly expressed in tumor-infiltrating lymphocytes (TILs) of various cancers including prostate cancer, renal cell carcinoma, colorectal cancer, and cervical cancer [29]. However, a comprehensive analysis of the expression of these ICRs in GC is lacking, especially regarding the expression status when considering intra-tumoral heterogeneity and clinicopathologic implications.

Recently, several targeted and immunotherapeutic agents were approved for palliative therapy in patients with recurrent or metastatic cancer. Based on the successful results of immune checkpoint inhibitors in trials of metastatic melanoma patients, a few new studies have evaluated the immunotherapeutic effects in high-risk resected stage III melanomas [30]. Although PD-1 inhibitors have shown therapeutic potential in various advanced cancers, including GC [13], the therapeutic response rates are still unsatisfactory, even in patients with PD-L1 expression [18]. To overcome this, recent studies have tried to employ immune checkpoint inhibitors for combination therapy, including combination with other immune checkpoint inhibitors, targeted agents, radiation, and conventional chemotherapeutic agents [31]. Importantly, the intracellular signaling pathway after interaction of PD-1 with PD-L1 is different from the intracellular pathways that are triggered upon binding of LAG3 and TIM3 to their specific ligands [32]. Dual blockade of PD-1 and LAG3 has been suggested to synergistically restore T cell function in cancer [33]. Previous studies have also suggested that PD-1 and TIM3 cooperate in the suppression of T cell responses and that their co-blockade results in greater

reinvigoration of effector T cell responses [34]. However, the co-expression status of various ICRs has not been clarified. Therefore, a comprehensive investigation of the immune microenvironment is necessary for managing cancer patients.

Immunotherapeutic agents are not only used for palliative therapy. For example, clinical trials are underway to combine cisplatin and 5-FU, the first-line therapy for patients with advanced GC, for neoadjuvant or adjuvant treatment [35]. In addition, chemotherapy reportedly has an effect on the tumor microenvironment (TME). Chemotherapy activates the immune response to tumors by strengthening the response of cytotoxic T cells, increasing antigenicity to cancer, or inhibiting immunosuppressive pathways [36, 37]. However, there are insufficient research results related to the expression pattern of ICRs, such as PD-1, and the co-expression of ICRs in patients with GC who are the targets of radical surgery. Therefore, the need for information on the expression of ICRs in patients with GC undergoing adjuvant chemotherapy after radical surgery or radical surgery after neoadjuvant chemotherapy is increasing.

1.2. Purpose of Research

In this study, HLA I molecules, such as HLA A/B/C and β2M, and the expression status of ICRs, such as PD-1, TIM3, and LAG3 in TIICs was evaluated by single immunohistochemistry (IHC) in patients with stage II and III GC to determine their clinicopathologic implications and prognostic significance. I also investigated the density of various immune cells, such as $CD8^+$ cytotoxic T cells, and molecular characteristics, such as EBV infection and MSI, to determine their relationship with the HLA I and ICRs expression status. Finally, I analyzed ICRs' expression based on immune cell context and their co-expression using multiplex immunohistochemistry (mIHC) in stage II and III GCs.

Chapter 2. Materials and methods

2.1. Patients and samples

A total of 406 patients with stage II and III GC who underwent curative radical surgery (R0 resection) with D2 lymph node dissection at Seoul National University Bundang Hospital (Seongnam-si, Republic of Korea) between 2006 and 2013 were screened in this study. Among them, cases of tissue samples inappropriate for IHC were excluded from the study. Patients who received fluoropyrimidine-based adjuvant chemotherapy after surgical resection were included. Clinicopathologic features, including overall survival (OS) and progression-free survival (PFS), were obtained from medical records and pathology reports, retrospectively.

Formalin-fixed paraffin-embedded (FFPE) tissue was collected from surgically resected GC specimens. In all cases, two separate 2-mm cores were selected from both the center and invasive margin of the tumor. Tissue microarray (TMA) blocks were designed as described previously (SuperBioChips Laboratories, Seoul, Republic of Korea) [38].

In addition, I prepared frozen sections from fresh tumor tissue and matched non-neoplastic gastric mucosa tissue samples that were obtained immediately from surgical specimens isolated from 6 gastric cancer patients, and FFPE sections were also produced. Both frozen sections and FFPE sections were produced in whole section slides.

2.2. Single IHC

All antibodies and staining devices used for single IHC are listed in Table 1

Table 1. List of antibodies and stainer devices used for single immunohistochemistry

Antibody	Clone	Species	Type	Dilution	Source	Stainer
PD-1	D4W2J	rabbit	monoclonal	1:100	Cell Signaling Technology[1]	BenchMark XT[2]
TIM3	D5D5R	rabbit	monoclonal	1:100	Cell Signaling Technology[1]	BenchMark XT[2]
LAG3	17B4	mouse	monoclonal	1:100	Abcam[3]	BenchMark XT[2]
HLA class I A/B/C	EMR8-5	mouse	monoclonal	1:8000	Abcam[3]	BenchMark XT[2]
β2M	r*B*2M/961	mouse	monoclonal	1:2000	Abcam[3]	BenchMark XT[2]
PD-L1[4]	22C3	mouse	monoclonal	-	Dako[5]	Autostainer Link 48[6]
p53	DO7	mouse	monoclonal	-	Dako[5]	BenchMark XT[2]
HER2	4B5	rabbit	monoclonal	predilution	Ventana[7]	BenchMark XT[2]
CD3	-	rabbit	Polyclonal	1:100	Dako[5]	BenchMark XT[2]
CD4	sp35	rabbit	monoclonal	-	Ventana[7]	BenchMark XT[2]
CD8	C8/114B	mouse	monoclonal	-	Dako[5]	BenchMark XT[2]

FOXP3	236A/E7	mouse	monoclonal	1:50	Abcam[3]	BenchMark XT[2]
CD68	PG-M1	mouse	monoclonal	1:100	Dako[5]	BenchMark XT[2]
CD163	10D6	mouse	monoclonal	1:100	Novocastra[8]	BenchMark XT[2]
E-cadherin	clone 36	mouse	monoclonal		BD Biosciences[9]	BenchMark XT[2]

PD-1, Programmed cell death-1; TIM-3, T-cell immunoglobulin and mucin domain-3; LAG-3, Lymphocyte activation gene-3; HLA, Human leukocyte antigen; β2M, Beta-2-microglobulin; PD-L1, Programmed cell death-ligand 1

[1] Danvers, MA, USA; [2] Ventana Medical Systems, Tucson, AZ, USA; [3] Cambridge, UK; [4] PharmDx kit; [5] Carpinteria, CA, USA; [6] Agilent, Santa Clara, CA, USA; [7] Tucson, AZ, USA; [8] Newcastle, UK; [9] San Jose, CA

2.3. Interpretation of HLA I molecule expression

HLA A/B/C and β2M expression was examined to determine the extent (%) and intensity of tumor cell membrane staining. The intensity was classified into the following three categories: 0, negative; 1+, weak positive; 2+, strong positive [24, 39]. For statistical analysis, I defined intact expression if more than 5% of tumor cells showed intensity of staining.

2.4. Interpretation of PD-1, TIM3, and LAG3 expression

PD-1, LAG3, and TIM3 expression was observed in the membranes with or without cytoplasm of tumor-infiltrating immune cells (TIICs), and interpreted as the extent (%) of immunostained TIICs. Positive expression was defined as immunostaining ≥ 5% of the immune cells [40].

2.5. Interpretation of PD-L1, E-cadherin, p53, and HER2 expression

PD-L1 expression was evaluated using the combined positive score (CPS) method. The cases were considered PD-L1^{+} if the CPS was one or more [40].

For E-cadherin, strong staining on the membrane of tumor cells was defined as positive expression, and if membrane staining was completely lost or abnormal cytoplasmic staining was observed, it was evaluated as altered expression.

For p53 expression in tumor cells, strong nuclear staining in 10% or more of the cells was interpreted as p53 overexpression/positive, and cases with less than 10% positive cells, including those showing scattered positive or patchy positive cells, were considered negative [41].

HER2 protein expression was assessed based on the staining intensity of tumor cell membranes. The scoring was classified into four categories based on the intensity of membrane staining (0 or 1+, negative; 2+, equivocal; 3+, positive), if 10% or

more tumor cells were stained [42].

2.6. Evaluation of immune cell density for CD3, CD4, CD8, Foxp3, CD68, and CD163 expression

All immunostained TMA slides were digitally scanned using an X400 Aperio ScanScope CS instrument (Aperio Technologies, Vista, CA, USA). The cell densities (number of positively stained cells per mm^2) in each core of the TMA slides were determined using an Aperio image analysis system (Leica Biosystems, New Castle, UK) [24].

2.7. MSI analysis

DNA extraction and polymerase chain reaction (PCR) of 5 National Cancer Institute (NCI) markers (BAT-26, BAT-25, D5S346, D17S250, and S2S123) were performed in both tumor cells and matched normal samples. PCR products from the FFPE samples were analyzed with an automatic sequencer (ABI 3731 Genetic Analyzer; Applied Biosystems, Foster City, CA, USA) according to a previously described protocol [43]. MSI status was assessed by comparing the allele profiles of two unstable marker as MSI-H, one unstable marker as MSI-low (MSI-L), and no unstable marker as microsatellite stable (MSS).

2.8. EBV in situ hybridization (ISH)

To determine the EBV status of tumor cells, EBV ISH was performed using an INFORM EBV-encoded RNA probe (Ventana Medical Systems, Tucson, AZ, USA). GC samples with cancer cells positive for nuclear EBER were considered EBV-positive.

2.9. Molecular classification in GC

I classified the GC samples used in the study into five subgroups (EBV+, MSI-H, epithelial-mesenchymal transition (EMT)-like, p53+, and p53-) using E-cadherin and p53 IHC, EBV ISH, and MSI status [43].

2.10 mIHC for ICRs and immune cells

I performed mIHC on TMA slides composed of 58 samples selected from the center of the tumor among the total GC samples. All implementations and analysis of mIHC were performed on the SuperBioChips (SuperBioChips Laboratories, Seoul, Korea). All antibodies and reagents used for mIHC are listed in Table 2. First, Harris hematoxylin (Merck, Darmstadt, Germany) was used for nuclear staining. After incubation with the primary antibody (Table 2) and washing twice with wash buffer (Dako, Carpinteria, CA, USA), the Envision FLEX + mouse linker/rabbit linker (Dako, Carpinteria, CA, USA) was treated with a secondary reagent. For chromogenic reaction and visualization, ImmPACT NovaRED (Vector Laboratories, Burlingame, CA, USA) was used. Mayer's hematoxylin (Dako, Carpinteria, CA, USA) was used for nuclear counterstaining, and all stained slides were subjected to full slide scanning using an Aperio AT2 scanner (Leica Biosystems, Newcastle upon Tyne, UK). After scanning, the slides were treated with a stripping buffer (20% sodium dodecyl sulfate, 0.5 M Tris-HCl pH 6.8, β-mercaptoethanol, and distilled water) and then microwaved for antibody stripping. The staining-scanning-stripping process was repeated sequentially for each primary antibody (Table 2).

For analysis, each 2 mm core in the TMA was extracted using an image program. CellProfiler (ver. 3.1.8. Broad Institute, Cambridge, MA) was used to adjust the image position so that the TMA core images extracted from each of the stained slide images could be matched in exactly the same two-dimensional positions. Thus, a single cell in the core represented the minimum unit of analysis. Staining information such as staining intensity for all primary antibodies in single cells was provided as a continuous variable. To assess the positive or negative status of all immunostained markers in each single cell, an appropriate cut-off value for staining intensity was determined (Table 2). Cytokeratin staining images

Table 2. Primary antibodies information for multiplex immunohistochemistry

Order	Antibody	Clone	Source	Cut-off
1	PD-1	D4W2J	Cell Signaling Technology	0.45
2	TIM3	D5D5R	Cell Signaling Technology	0.3
3	LAG3	17B4	Abcam	0.4
4	CD8	SP57	Ventana	0.3
5	CD3	Polyclonal	Dako	0.35
6	FOXP3	236A/E7	Abcam	0.3
7	CD68	PG-M1	Dako	0.4
8	CK	AE1/AE3	Dako	0.35

PD-1, Programmed cell death-1; TIM-3, T-cell immunoglobulin and mucin domain-3; LAG-3, Lymphocyte activation gene-3; CK, Cytokeratin

were used to evaluate each stained cell separately from the intratumoral and stromal areas. The density of positive cells in stained cells was defined as the number of positive cells per mm2. More detailed information on mIHC procedures has been provided in previous studies [44].

2.11 Statistical analysis

All analyses were performed using R 4.1.1, RStudio 1.3.1093, and SPSS 25.0 (SPSS, Inc., Chicago, IL, USA). For single IHC, Pearson's chi-square test was used to analyze the association among ICRs, HLA A/B/C, β2m, molecular classification markers, and clinicopathologic features. In addition, the McNemar test was used to examine intratumor ICR heterogeneity between tumor centers and peripherals. The association between ICRs and immune cell density was determined using the Pearson correlation coefficient. OS was analyzed using the Kaplan–Meier method and log-rank test, and independent prognostic factors were identified by univariate and multivariate Cox regression analyses.

For mIHC, the Wilcoxon rank-sum test was used to identify statistical significance between two groups, and comparison between multiple groups was performed using the Kruskal-Wallis test with Bonferroni correction in the R function wilcox_test() from the package "rstatix" (Alboukadel Kassambara, 2020, rstatix: Pipe-friendly framework for basic statistical tests. R package version 0.4.0; https://cran.r-project.org/web/packages/rstatix/index.html). Box and whisker plots were used to show the median and quartiles. To determine the ideal cut-off values for establishing high and low cell density groups, I used the 'surv_cutpoint()' function from the package "survminer" (Alboukadel Kassambara (2019), survminer: Drawing Survival Curves using 'ggplot2'. R package version 0.4.6; https://cran.r-project.org/web/packages/survminer/index.html) using the maximally selected rank statistic from the 'maxstat' R package [45]. Following this analysis, the 'analyse_multivariate()' function using Cox regression analysis and 'forest plot()' function

from the package “survivalAnalysis” (Marcel Wiesweg (2019), survivalAnalysis: High-Level Interface for Survival Analysis and Associated Plots. R package version 0.1.1; https://cran.r-project.org/web/packages/survivalAnalysis/index.html) was used to perform univariate survival analysis for immune cell and immune checkpoint expressing cell and to create forest plots for each parameter. For cluster analysis, first, data standardization and log-2 transformation were performed, and unsupervised hierarchical clustering using an Euclidean distance measure and complete linkage was performed with the ‘hclust()’ function from the package “stats.” OS for clusters was determined using the Kaplan–Meier method and log-rank test. A probability value of less than 0.05 was considered statistically significant.

Chapter 3. Results

3.1. Clinicopathologic significance of HLA I and β2M expression

To reveal the clinicopathologic significance of HLA I molecules, I performed IHC for HLA A/B/C and β2M. Representative pictures are shown in Fig. 1. Of the 406 cases, 11 cases were excluded due to inadequate HLA A/B/C and β2M IHC results. Of the 395 cases, HLA A/B/C expression was lost in 210 cases (53.2%) in the tumor center and 210 cases (53.2%) in the invasive margin. HLA A/B/C expression in the tumor center was correlated with the invasive margin ($k = 0.502$, $p < 0.001$), and expression loss in either the center or invasive margin was observed in 258 cases (65.3%). β2M expression was lost in 177 (44.8%), 193 (48.9%), and 235 (59.5%) of cases in the center, invasive margin, and center or invasive margin, respectively. The kappa value between the center and invasive margin of β2M expression was 0.482 ($p < 0.001$). Both HLA A/B/C and β2M expression showed no definite predilection for the tumor center or invasive border. Additionally, HLA A/B/C expression loss in the center or invasive margin was closely associated with β2M expression loss in the center or invasive margin ($k = 0.683$, $p < 0.001$).

In the FFPE sections and frozen sections of 6 cases, when HLA A/B/C expression in the non-neoplastic gastric mucosa was compared with expression in tumor tissues, HLA A/B/C expression was found to be lost or downregulated in non-neoplastic gastric mucosa in frozen sections of all six cases and FFPE sections of five cases. The intensity and extent of HLA A/B/C expression was generally similar between the frozen and FFPE sections, but one case showed focal expression of HLA A/B/C in the frozen section and loss of HLA A/B/C expression in the FFPE section derived from tumor tissue (Fig. 2 and 3).

The correlations between clinicopathologic variables and

Figure 1. Representative figures showing intact expression of human leukocyte antigen (HLA) A/B/C (a), beta-2-microglobulin (β2M) (c) and expression loss of HLA A/B/C (b), β2M (d) (20× magnification).

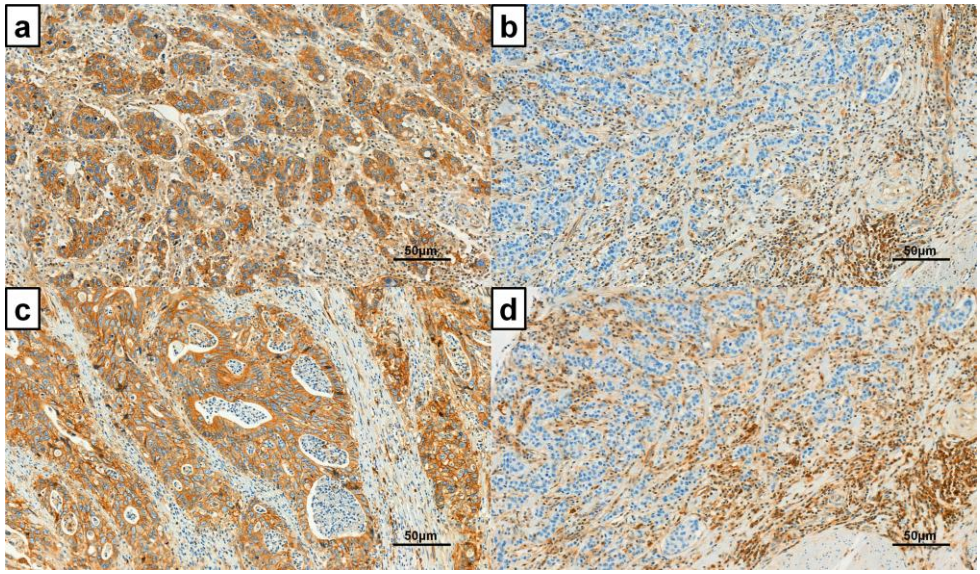

Figure 2. Comparison of human leukocyte antigen (HLA) A/B/C expression between non-neoplastic gastric mucosa and tumor tissue of frozen section (a) and of formalin-fixed paraffin-embedded (FFPE) section (b), and between frozen and FFPE sections of tumor tissues (c). HLA A/B/C expression was found to be lost or downregulated in non-neoplastic gastric mucosa of all six cases of frozen sections and five cases of FFPE sections. HLA A/B/C expression of frozen tumor tissue was generally similar as FFPE sections, but one case showed focal expression of HLA A/B/C in the frozen section and loss of HLA A/B/C expression in the FFPE section.

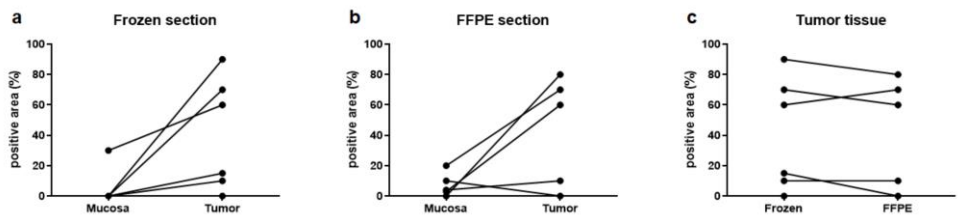

Figure 3. Representative figures showing loss of human leukocyte antigen (HLA) A/B/C expression in non-neoplastic gastric mucosa-derived frozen section (a) and formalin-fixed paraffin-embedded (FFPE) section (c) and strong intensity expression of HLA A/B/C in tumor-derived frozen section (b) and FFPE section (d) (20× magnification).

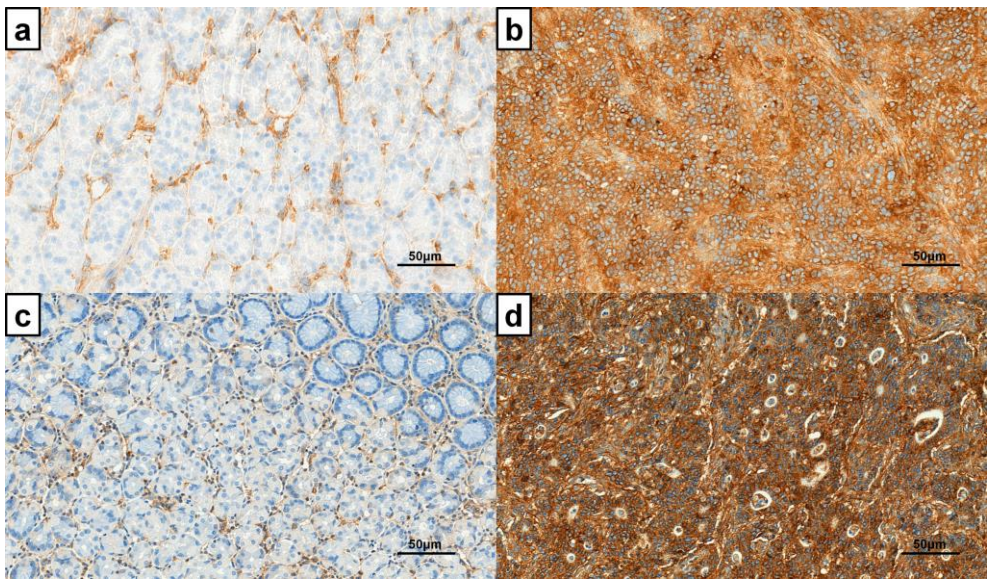

HLA I molecule expression are summarized in Table 3. Both HLA A/B/C and β2M expression loss were significantly associated with more aggressive clinicopathologic features, including poorly differentiated/poorly cohesive carcinoma (HLA A/B/C loss, $p = 0.001$; β2M loss, $p < 0.001$), diffuse histologic type by Lauren classification (HLA A/B/C, $p = 0.001$; β2M, $p = 0.002$), and infiltrative tumor border (all $p < 0.001$). β2M expression loss was significantly correlated with perineural invasion ($p = 0.013$), while HLA A/B/C loss did not show a significant correlation ($p = 0.096$). Additionally, I combined the expression status of HLA A/B/C and β2M, and expression loss of either HLA A/B/C or β2M was significantly associated with poorly differentiated/poorly cohesive carcinoma ($p < 0.001$), diffuse histologic type by Lauren classification ($p = 0.002$), and infiltrative tumor border ($p < 0.001$).

3.2. Correlation of HLA I expression with tumor microenvironment and molecular characteristics

I performed PD-L1 IHC and calculated CPS in each core in order to correlate the HLA I molecule expression status with the tumor microenvironment. Among the 395 cases, PD-L1 IHC was positive in 197 cases (49.9%) for the tumor center, 158 cases (40.0%) for the invasive margin, and 226 cases (57.2%) for either the center of tumor or invasive margin. When HLA A/B/C or β2M expression status was correlated with the PD-L1 expression status, intact HLA A/B/C and β2M expression was significantly correlated with positive PD-L1 expression ($p < 0.001$, Table 4). However, among 226 PD-L1+ GC cases, HLA A/B/C or β2M expression was lost in 138 cases (61.1%).

Correlations between HLA I molecule expression and ICRs such as PD-1, TIM3, and LAG3 expression were verified in 382 of 406 patients, except for 26 instances with insufficient HLA I molecule and ICRs IHC data. When HLA A/B/C or β2M expression status was correlated with the PD-1, TIM3 and LAG3 expression status, intact HLA A/B/C and β2M expression

Table 3. Correlation between clinicopathological features and human leukocyte antigen (HLA) A/B/C and beta-2-microglobulin (β2M) status in stage II, III gastric cancer

		HLA A/B/C			β2M			HLA A/B/C or β2M		
Characteristics	Total	Loss	Intact	p value	Loss	Intact	p value	Loss	Intact	p value
Age (years)				0.312			0.307			0.400
<65	261 (66.1%)	175 (67.8%)	86 (62.8%)		160 (68.1%)	101 (63.1%)		186 (67.4%)	75 (63.0%)	
≥65	134 (33.9%)	83 (32.2%)	51 (37.2%)		75 (31.9%)	60 (36.9%)		90 (32.6%)	44 (37.0%)	
Sex				0.049			0.047			0.033
Male	251 (63.5%)	155 (60.1%)	96 (70.1%)		140 (59.6%)	111 (69.4%)		166 (60.1%)	85 (71.4%)	
Female	144 (36.5%)	103 (39.9%)	41 (29.9%)		95 (40.4%)	49 (30.6%)		110 (39.9%)	34 (28.6%)	
pTNM				0.604			0.127			0.373
II	189 (47.8%)	121 (46.9%)	68 (49.6%)		105 (44.7%)	84 (52.5%)		128 (46.4%)	61 (51.3%)	
III	206 (52.2%)	137 (53.1%)	69 (50.4%)		130 (55.3%)	76 (47.5%)		148 (53.6%)	58 (48.7%)	
Tumor size				0.201			0.022			0.116
≤ 5cm	222 (56.2%)	139 (53.9%)	83 (60.6%)		121 (51.5%)	101 (63.1%)		148 (53.6%)	74 (62.2%)	
> 5cm	173 (43.8%)	119 (46.1%)	54 (39.4 %)		114 (48.5%)	59 (36.9%)		128 (46.4%)	45 (37.8%)	
Location				0.120			0.111			0.066
Upper third	184 (46.6%)	112 (43.4%)	72 (52.6%)		98 (41.7%)	86 (53.8%)		121 (43.8%)	63 (52.9%)	

Middle third	84 (21.3%)	61 (23.6%)	23 (16.8%)		56 (23.8%)	28 (17.5%)		62 (22.5%)	22 (18.5%)	
Lower third	104 (26.3%)	70 (27.1%)	34 (24.8%)		65 (27.7%)	39 (24.4%)		74 (26.8%)	30 (25.2%)	
GEJ	6 (1.5%)	2 (0.8%)	4 (2.9%)		3 (1.3%)	3 (1.8%)		3 (1.1%)	3 (2.5%)	
Entire	17 (4.3%)	13 (5.1%)	4 (2.9%)		13 (5.5%)	4 (2.5%)		16 (5.8%)	1 (0.9%)	
WHO				0.001			<0.001			<0.001
WD	5 (1.3%)	3 (1.2%)	2 (1.5%)		1 (0.4%)	4 (2.5%)		3 (1.1%)	2 (1.7%)	
MD	124 (31.4%)	68 (26.4%)	56 (40.9%)		64 (27.2%)	60 (37.5%)		77 (27.9%)	47 (39.5%)	
PD	164 (41.5%)	112 (43.4%)	52 (38.0%)		95 (40.4%)	69 (43.1%)		115 (41.7%)	49 (41.2%)	
PCC(SRC)	96 (24.3%)	74 (28.7%)	22 (16.1%)		74 (31.5%)	22 (13.8%)		80 (29.0%)	16 (13.4%)	
UD	1 (0.3%)	0 (0.0%)	1 (0.7%)		0 (0.0%)	1 (0.6%)		0 (0.0%)	1 (0.8%)	
GCLS/ADSQCA	5 (1.2%)	1 (0.3%)	4 (2.8%)		1 (0.5%)	4 (2.5%)		1 (0.3%)	4 (3.4%)	
Lauren classification				0.001			0.002			0.002
Intestinal	144 (36.5%)	81 (31.4%)	63 (46.0%)		71 (30.2%)	73 (45.6%)		90 (32.6%)	54 (45.4%)	
Diffuse	219 (55.4%)	161 (62.4%)	58 (42.3%)		148 (63.0%)	71 (44.4%)		169 (61.2%)	50 (42.0%)	
Mixed	30 (7.6%)	15 (5.8%)	15 (10.9%)		15 (6.4%)	15 (9.4%)		16 (5.8%)	14 (11.8%)	
Indeterminate	2 (0.5%)	1 (0.4%)	1 (0.8%)		1 (0.4%)	1 (0.6%)		1 (0.4%)	1 (0.8%)	

Ming's classification				<0.001			<0.001			<0.001
Infiltrative	320 (81.0%)	227 (88.0%)	93 (67.9%)		207 (88.1%)	113 (70.6%)		243 (88.0%)	77 (64.7%)	
Expanding	75 (19.0%)	31 (12.0%)	44 (32.1%)		28 (11.9%)	47 (29.4%)		33 (12.0%)	42 (35.3%)	
Lymphatic invasion				0.171			0.822			0.411
Absent	121 (30.6%)	85 (32.9%)	36 (26.3%)		73 (31.1%)	48 (30.0%)		88 (31.9%)	33 (27.7%)	
Present	274 (69.4%)	173 (67.1%)	101 (73.7%)		162 (68.9%)	112 (70.0%)		188 (68.1%)	86 (72.3%)	
Vascular invasion				0.884			0.754			0.419
Absent	333 (84.3%)	217 (84.1%)	116 (84.7%)		197 (83.8%)	136 (85.0%)		230 (83.3%)	103 (86.6%)	
Present	62 (15.7%)	41 (15.9%)	21 (15.3%)		38 (16.2%)	24 (15.0%)		46 (16.7%)	16 (13.4%)	
Perineural invasion				0.096			0.013			0.121
Absent	137 (34.7%)	82 (31.8%)	55 (40.1%)		70 (29.8%)	67 (41.9%)		89 (32.2%)	48 (40.3%)	
Present	258 (65.3%)	176 (68.2%)	82 (59.9%)		165 (70.2%)	93 (58.1%)		187 (67.8%)	71 (59.7%)	
Total	395	258 (65.3%)	137 (34.7%)		235 (59.5%)	160 (40.5%)		276 (69.9%)	119 (30.1%)	

Abbreviations GEJ, gastroesophageal junction; WD, well differentiated; MD, moderately differentiated; PD, poorly differentiated; PCC(SRC), poorly cohesive carcinoma (signet ring cell carcinoma); GCLS, gastric carcinoma with lymphoid stroma; UD, undifferentiated carcinoma; ADSQCA, adenosquamous carcinoma

Table 4. Correlation human leukocyte antigen (HLA) I expression, such as HLA A/B/C and beta-2-microglobulin (β2M), and PD-L1/PD-1, TIM3 and LAG3 in stage II, III gastric cancer.

Characteristics		Total	HLA A/B/C			β2M			HLA A/B/C or β2M		
			Loss	Intact	p value	Loss	Intact	p value	Loss	Intact	p value
PD-L1 CT or IM	Negative	169 (42.8%)	127 (49.2%)	42 (30.7%)	<0.001	122 (51.9%)	47 (29.4%)	<0.001	138 (50.0%)	31 (26.1%)	<0.001
	Positive	226 (57.2%)	131 (50.8%)	95 (69.3%)		113 (48.1%)	113 (70.6%)		138 (50.0%)	88 (73.9%)	
PD-L1 CT	Negative	198 (50.1%)	148 (57.4%)	50 (36.5%)	<0.001	139 (59.1%)	59 (36.9%)	<0.001	160 (58.0%)	38 (31.9%)	<0.001
	Positive	197 (49.9%)	110 (42.6%)	87 (63.5%)		96 (40.9%)	101 (63.1%)		116 (42.0%)	81 (68.1%)	
PD-L1 IM	Negative	237 (60.0%)	178 (69.0%)	59 (43.1%)	<0.001	166 (70.6%)	71 (44.4%)	<0.001	190 (68.8%)	47 (39.5%)	<0.001
	Positive	158 (40.0%)	80 (31.0%)	78 (56.9%)		69 (29.4%)	89 (56.3%)		86 (31.2%)	72 (60.5%)	
Total		395	258 (65.3%)	137 (34.7%)		235 (59.5%)	160 (40.5%)		276 (69.9%)	119 (30.1%)	
PD-1	Negative	291 (76.2%)	217 (85.4%)	74 (57.8%)	<0.001	198 (86.5%)	93 (60.8%)	<0.001	232 (85.6%)	59 (53.2%)	<0.001
	Positive	91 (23.8%)	37 (14.6%)	54 (42.2%)		31 (13.5%)	60 (39.2%)		39 (14.4%)	52 (46.8%)	
TIM3	Negative	126 (33.0%)	97 (38.2%)	29 (22.7%)	0.003	95 (41.5%)	31 (20.3%)	<0.001	105 (38.7%)	21 (18.9%)	<0.001
	Positive	256 (67.0%)	157 (61.8%)	99 (77.3%)		134 (58.5%)	122 (79.7%)		166 (61.3%)	90 (81.1%)	
LAG3	Negative	189 (49.5%)	150 (59.1%)	39 (30.5%)	<0.001	142 (62.0%)	47 (30.7%)	<0.001	160 (59.0%)	29 (26.1%)	<0.001
	Positive	193	104	89		87	106		111	82	

	(50.5%)	(40.9%)	(69.5%)	(38.0%)	(69.3%)	(41.0%)	(73.9%)
Total	382	254 (66.5%)	128 (33.5%)	229 (59.9%)	153 (40.1%)	271 (70.9%)	111 (29.1%)

Abbreviations PD-L1, Programmed death-ligand 1; CT, center of tumor; IM, invasive margin; PD-1, Programmed cell death-1; TIM-3, T-cell immunoglobulin and mucin domain-3; LAG-3, Lymphocyte activation gene-3

showed a significant correlation with PD-1, TIM3 and LAG3-positive expression (all $p < 0.001$, Table 4). However, among 91 PD-1+, 256 TIM3+ and 193 LAG3+ GC cases, HLA A/B/C or β2M expression was lost in 39 PD-1+ cases (42.9%), 166 TIM3+ (64.8%) and 111 LAG3+ (57.5%) cases, respectively.

The number of tumor-infiltrating $CD8^+$ cytotoxic T cells ranged from (2.79- 1222.93) cells/mm^2 with a median value of 219.92 cells/mm^2 for the center of the tumor and (6.90-1374.94) cells/mm2 with a median value of 195.75 cells/mm^2 for the invasive margin. $CD8^+$ cytotoxic T cell density was significantly higher in cases with the intact expression of HLA A/B/C and β2M. In contrast, the density was significantly lower when HLA A/B/C or β2M expression was lost (all $p < 0.001$, Fig. 4).

Expression loss of HLA A/B/C and β2M was inversely correlated with EBV positivity in GCs (all $p < 0.001$, Table 5). Expression of HLA A/B/C and β2M tended to be intact in EBV-positive GCs. Expression loss of HLA A/B/C and β2M showed no significant correlation with p53 overexpression (HLA A/B/C, $p = 0.971$; β2M, $p = 0.559$) or MSI status (HLA A/B/C, $p = 0.432$; β2M, $p = 0.748$). Among the 37 MSI-H cases, HLA A/B/C expression was lost in 22 (59.5%) cases, and β2M expression was lost in 21 (56.8%) cases. Although HLA I expression loss was infrequently found in EBV-positive GCs (5 of 26 cases, 19.2%), MSI-H GCs showed frequent loss of HLA I molecules expression (25 or 37 cases, 67.6%).

3.3. Prognostic significance of HLA I molecule expression

According to Kaplan-Meier survival analysis, patients with expression loss of both HLA A/B/C and β2M had significantly worse outcomes (HLA A/B/C loss, $p = 0.019$; Fig. 5a; β2M loss, $p = 0.009$; Fig. 5b). Loss of either HLA A/B/C or β2M expression was also significantly associated with worse OS compared to the intact HLA A/B/C and β2M expression group ($p = 0.003$, Fig. 5c).

Figure 4. Association between CD8+ cytotoxic T cell infiltration and expression of human leukocyte antigen (HLA) A/B/C (a, b) and beta-2-microglobulin (β2M) (c, d) and either HLA A/B/C or β2M (e, f) in the center of the tumor (CT) (a, c, e) and invasive margin (IM) (b, d, f). CD8+ cytotoxic T cell density was significantly higher in cases with the intact expression of HLA A/B/C and β2M. In contrast, it was significantly lower when HLA A/B/C or β2M expression was lost in either center of the tumor or the invasive margin ($p < 0.001$ in all cases).

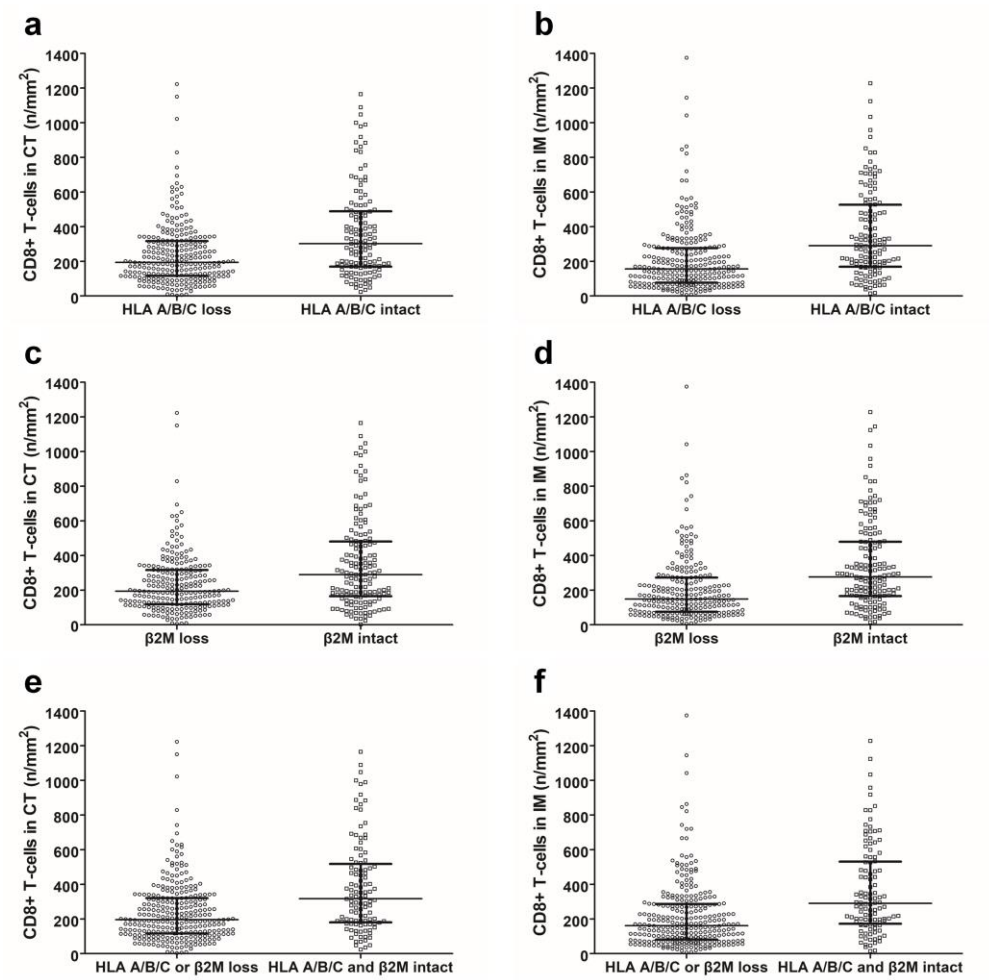

Table 5. Correlation human leukocyte antigen (HLA) A/B/C and beta-2-microglobulin (β2M) expression and molecular characteristics in stage II, III gastric cancer

Characteristics		Total	HLA A/B/C			β2M			HLA A/B/C or β2M		
			Loss	Intact	p value	Loss	Intact	p value	Loss	Intact	p value
EBV	Negative	369 (93.4%)	253 (98.1%)	116 (84.7%)	<0.001	231 (98.3%)	138 (86.3%)	<0.001	271 (98.2%)	98 (82.4%)	<0.001
	Positive	26 (6.6%)	5 (1.9%)	21 (15.3%)		4 (1.7%)	22 (13.8%)		5 (1.8%)	21 (17.6%)	
p53	Negative	285 (72.2%)	186 (72.1%)	99 (72.3%)	0.971	167 (71.1%)	118 (73.8%)	0.559	198 (71.7%)	87 (73.1%)	0.780
	Positive	110 (27.8%)	72 (27.9%)	38 (27.7%)		68 (28.9%)	42 (26.2%)		78 (28.3%)	32 (26.9%)	
MSI	MSS/MSI-L	358 (90.6%)	236 (91.5%)	122 (89.1%)	0.432	214 (91.1%)	144 (90.0%)	0.722	251 (90.9%)	107 (89.9%)	0.748
	MSI-H	37 (9.4%)	22 (8.5%)	15 (10.9%)		21 (8.9%)	16 (10.0%)		25 (9.1%)	12 (10.1%)	
Total		395	258 (65.3%)	137 (34.7%)		235 (59.5%)	160 (40.5%)		276 (69.9%)	119 (30.1%)	

Abbreviations CT, center of tumor; IM, invasive margin; MSS, microsatellite stable; MSI-L, microsatellite instability-low; MSI-H, microsatellite instability-high

Figure 5. Kaplan–Meier survival curves showing the prognostic value of human leukocyte antigen (HLA) A/B/C and beta-2-microglobulin (β2M) expression in gastric cancer. Loss of HLA A/B/C (a) and β2M (b) was associated with poor overall survival (p = 0.019 and p = 0.009, respectively). Loss of either HLA A/B/C or β2M (c) expression was also significantly associated with poor overall survival when compared with intact HLA A/B/C and β2M expression (p = 0.003).

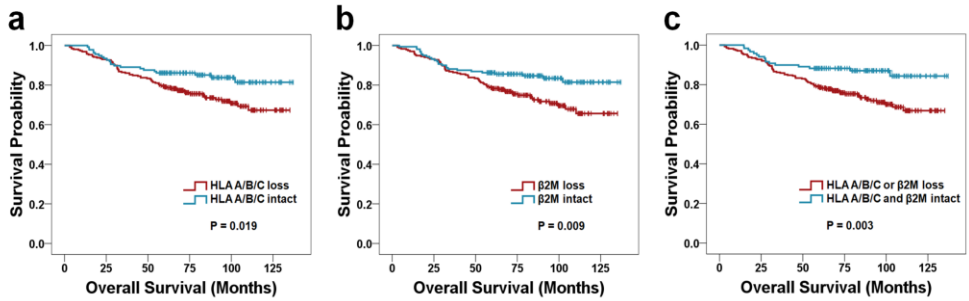

Univariate analysis indicated that loss of either HLA A/B/C or β2M expression and established prognostic factors, including age, tumor size, pathologic stage, vascular invasion, and perineural invasion, were significantly associated with OS (Table 6). According to multivariate analysis, loss of either HLA A/B/C or β2M expression was identified as an independent unfavorable prognostic factor for OS (hazard ratio 1.946; 95% confidence interval 1.131−3.350; p = 0.016). Age, tumor size, pTNM stage, vascular invasion, and perineural invasion were also significantly independent prognostic factors for OS (age, p = 0.046; size, p = 0.019; pTNM, p = 0.009; vascular invasion, p = 0.002; perineural invasion, p = 0.028).

3.4. Clinicopathologic and prognostic significance of ICR expression

ICRs expression was evaluated in 385 cases out of a total of 406 cases, excluding 21 cases with inadequate ICRs IHC results. Representative pictures are shown in Fig. 6. Of the 385 stage II and III GCs, 68 cases (17.7%) showed positive PD−1 expression in the center, 69 (17.9%) in the invasive margin, and 91 (23.6%) in the center or invasive margin. LAG3 expression was found in 175 (45.5%), 114 (29.6%), and 193 (50.1%), and TIM3 in 237 (61.6%), 134 (34.8%), and 257 (66.8%) cases in the center, invasive margin, and center or invasive margin, respectively. PD−1 expression was similar between the center and invasive margin (p = 1.0, McNemar test; Table 7). However, LAG3 and TIM3 expression levels were significantly higher in the center than in the invasive margin (p < 0.001 by McNemar test). The rate of agreement, Cohen's κ values, and the correlation coefficient of PD−1 expression between the center and invasive margin were higher than those of LAG3 and TIM3 (Table 7). The clinicopathologic features are summarized in Table 8. PD−1 expression was associated with old age, expanding growth, and distal location (p < 0.05), LAG3 expression with expanding growth and distal location (p < 0.05), and TIM3 expression with infiltrative growth, unlike PD−1 and LAG3 (p <

Table 6. Univariate and multivariate survival analysis by using Cox-regression analysis for human leukocyte antigen A/B/C and beta-2-microglobulin expression

Variable	Univariate			Multivariate		
	HR	95% CI	*P*	HR	95% CI	*P*
Age (years) (≥ 65 vs. < 65*)	1.878	1.243 – 2.839	0.003	1.540	1.131 – 3.350	0.046
Sex (Female vs. male*)	0.767	0.506 – 1.163	0.212	–	–	–
Tumor size (> 5cm vs. ≤ 5cm*)	2.617	1.702 – 4.026	<0.001	1.718	1.094 – 2.699	0.019
pTNM stage (III vs. II*)	3.706	2.255 – 6.089	<0.001	2.076	1.202 – 3.584	0.009
Lauren classification (Non-intestinal vs. intestinal*)	1.429	0.906 – 2.252	0.124	–	–	–
Ming classification (Infiltrative vs. expanding*)	1.844	0.982 – 3.464	0.057	–	–	–
Lymphatic invasion (Present vs. absent*)	1.528	0.938 – 2.489	0.088	–	–	–
Vascular invasion (Present vs. absent*)	3.519	2.278 – 5.437	<0.001	2.097	1.326 – 3.317	0.002
Perineural invasion (Present vs. absent*)	3.187	1.803 – 5.634	<0.001	1.969	1.077-3.600	0.028
Loss of HLA A/B/C or β2M (Loss vs. intact*)	2.191	1.277 – 3.761	0.004	1.946	1.131 – 3.350	0.016

* Reference variable;

Figure 6. Representative figures showing the positive expression of programmed cell death protein 1 (PD−1) (a), T cell immunoglobulin and mucin domain 3 (TIM3) (b) and lymphocyte activation gene−3 (LAG3), as well as the negative expression of PD−1 (d), TIM3 (e) and LAG3 (f) by single immunohistochemistry (20× magnification).

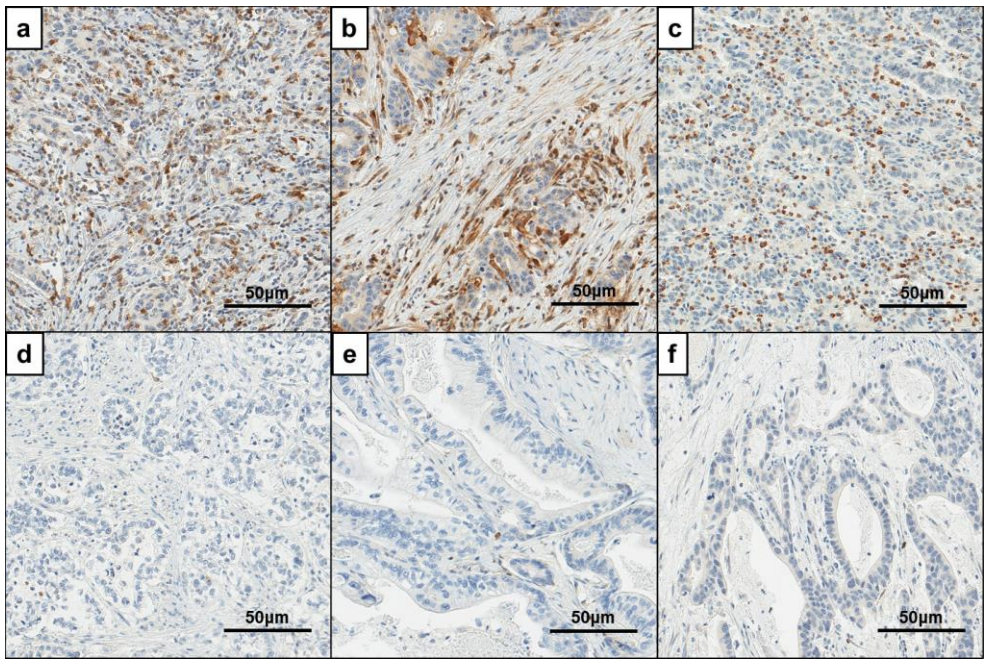

Table 7. Intratumoral heterogeneity of immune checkpoints expression between center and periphery

			Periphery					
			Negative	Positive	p value*	Agreement (%)	Cohen's kappa (lower 95% CI)	CC
Center	PD-1				1.000	88.31	0.600	0.625**
		Negative	294 (76.4%)	23 (6.0%)				
		Positive	22 (5.7%)	46 (11.9%)				
	LAG-3				<0.001	74.81	0.477	0.505**
		Negative	192 (49.9%)	18 (4.7%)				
		Positive	79 (20.5%)	96 (24.9%)				
	TIM-3				<0.001	62.86	0.306	0.353**
		Negative	128 (33.2%)	20 (5.3%)				
		Positive	123 (31.9%)	114 (29.6%)				

* by McNemar test; ** p value < 0.01; CC, Correlation coefficient; PD-1, Programmed cell death-1; CK, Cytokeratin; TIM-3, T-cell immunoglobulin and mucin domain-3; LAG-3, Lymphocyte activation gene-3

Table 8. Correlation between immune checkpoint receptors and clinicopathologic features

Characteristics		Total	PD-1			LAG-3			TIM-3		
			Negative	Positive	p value	Negative	Positive	p value	Negative	Positive	p value
Age					0.016			0.126			0.591
	median (range)	59.0 (20-87)	58.0 (20-87)	62.0 (31-82)		57.5 (20-87)	59.0 (28-85)		58.0 (22-87)	59.0 (20-85)	
Sex					0.082			0.023			0.631
	Male	250 (64.9%)	184 (62.6%)	66 (72.5%)		114 (59.4%)	136 (70.5%)		81 (63.3%)	169 (65.8%)	
	Female	135 (35.1%)	110 (37.4%)	25 (27.5%)		78 (40.6%)	57 (29.5%)		47 (36.7%)	88 (34.2%)	
Size					0.327			0.106			0.209
	median (range)	4.9 (1.2-20.0)	4.6 (1.2-20.0)	5.3 (1.4-12.0)		5.0 (1.4-20.0)	4.5 (1.2-17.5)		5.1 (1.5-20.0)	4.7 (1.2-17.5)	
Lauren					<0.001			<0.001			0.004
	Intestinal	143 (37.1%)	104 (35.4%)	39 (42.9%)		62 (32.3%)	81 (42.0%)		42 (32.8%)	101 (39.3%)	
	Diffuse	212 (55.1%)	175 (59.5%)	37 (40.7%)		123 (64.1%)	89 (46.1%)		83 (64.8%)	129 (50.2%)	
	Mixed	29 (7.5%)	15 (5.1%)	14 (15.4%)		7 (3.6%)	22 (11.4%)		3 (2.4%)	26 (10.1%)	
	Indeterminate	1 (0.3%)	0 (0.0%)	1 (1.0%)		0 (0.0%)	1 (0.5%)		0 (0.0%)	1 (0.4%)	
WHO Classification					0.003			0.011			0.098
	Papillary	2 (0.5%)	2 (0.7%)	0 (0.0%)		2 (1.0%)	0 (0.0%)		0 (0.0%)	2 (0.8%)	

WD	5 (1.3%)	4 (1.4%)	1 (1.1%)		3 (1.6%)	2 (1.0%)		2 (1.6%)	3 (1.2%)	
MD	119 (30.9%)	90 (30.6%)	29 (31.9%)		51 (26.6%)	68 (35.2%)		34 (26.6%)	85 (33.1%)	
PD	148 (38.4%)	107 (36.4%)	41 (45.1%)		70 (36.5%)	78 (40.4%)		47 (36.7%)	101 (39.3%)	
Mucinous	13 (3.4%)	11 (3.7%)	2 (2.2%)		5 (2.6%)	8 (4.1%)		4 (3.1%)	9 (3.5%)	
SRC	46 (11.9%)	40 (13.6%)	6 (6.6%)		30 (15.6%)	16 (8.3%)		16 (12.5%)	30 (11.7%)	
PCC	47 (12.2%)	40 (13.6%)	7 (7.7%)		31 (16.1%)	16 (8.3%)		25 (19.5%)	22 (8.6%)	
UD	1 (0.3%)	0 (0.0%)	1 (1.1%)		0 (0.0%)	1 (0.5%)		0 (0.0%)	1 (0.4%)	
GCLS	4 (1.0%)	0 (0.0%)	4 (4.4%)		0 (0.0%)	4 (2.1%)		0 (0.0%)	4 (1.6%)	
Ming Classification				<0.001			<0.001			<0.001
Infiltrative	320 (83.1%)	268 (91.2%)	52 (57.1%)		178 (92.7%)	142 (73.6%)		119 (93.0%)	201 (78.2%)	
Expanding	65 (16.9%)	26 (8.8%)	39 (42.9%)		14 (7.3%)	51 (26.4%)		9 (7.0%)	56 (21.8%)	
Lymphatic invasion				0.093			0.07			0.129
Absent	116 (30.1%)	95 (32.3%)	21 (23.1%)		66 (34.4%)	50 (25.9%)		45 (35.2%)	71 (27.6%)	
Present	269 (69.9%)	199 (67.7%)	70 (76.9%)		126 (65.6%)	143 (74.1%)		83 (64.8%)	186 (72.4%)	
Vascular invasion				0.589			0.982			0.635
Absent	323 (83.9%)	245 (83.3%)	78 (85.7%)		161 (83.9%)	162 (83.9%)		109 (85.2%)	214 (83.3%)	

	Present	62 (16.1%)	49 (16.7%)	13 (14.3%)		31 (16.1%)	31 (16.1%)		19 (14.8%)	43 (16.7%)	
Perineural invasion					0.003			0.056			0.557
	Absent	128 (33.2%)	86 (29.3%)	42 (46.2%)		55 (28.6%)	73 (37.8%)		40 (31.3%)	88 (34.2%)	
	Present	257 (66.8%)	208 (70.7%)	49 (53.8%)		137 (71.4%)	120 (62.2%)		88 (68.8%)	169 (65.8%)	
Location					0.016			<0.001			0.26
	Lower	180 (46.8%)	129 (43.9%)	51 (56.0%)		73 (38.0%)	107 (55.4%)		56 (43.8%)	124 (48.2%)	
	Middle	81 (21.0%)	73 (24.8%)	8 (8.8%)		55 (28.6%)	26 (13.5%)		31 (24.2%)	50 (19.5%)	
	Upper	102 (26.5%)	75 (25.5%)	27 (29.7%)		52 (27.1%)	50 (25.9%)		33 (25.8%)	69 (26.8%)	
	GEJ	5 (1.3%)	3 (1.0%)	2 (2.2%)		1 (0.5%)	4 (2.1%)		0 (0.0%)	5 (1.9%)	
	Whole	17 (4.4%)	14 (4.8%)	3 (3.3%)		11 (5.7%)	6 (3.1%)		8 (6.3%)	9 (3.5%)	
pTNM					0.555			0.876			0.294
	II	180 (46.8%)	135 (45.9%)	45 (49.5%)		89 (46.4%)	91 (47.2%)		55 (43.0%)	125 (48.6%)	
	III	205 (53.2%)	159 (54.1%)	46 (50.5%)		103 (53.6%)	102 (52.8%)		73 (57.0%)	132 (51.4%)	
Total		385	294 (76.4%)	91 (23.6%)		192 (49.9%)	193 (50.1%)		128 (33.2%)	257 (66.8%)	

PD-1, Programmed cell death-1; TIM-3, T-cell immunoglobulin and mucin domain-3; LAG-3, Lymphocyte activation gene-3; WD, Well differentiated; MD, Moderately differentiated; PD, Poorly differentiated; SRC, Signet ring cell carcinoma; PCC, Poorly cohesive carcinoma; UD, Undifferentiated carcinoma; GCLS, Gastric carcinoma with lymphoid stroma; GEJ, Gastroesophageal junction

0.05). In addition, TIM3−expressing cases showed more diffuse−type in positive expression than in negative expression when compared with PD−1− and LAG3−expressing cases.

Kaplan−Meier survival analysis showed that GC patients with positive expression of PD−1, TIM3, and LAG3 in the center, invasive margin, and center or invasive margin tended to have better OS than those with negative expression (Fig. 7), but the difference was only statistically significant in cases where LAG3 was expressed in the invasive margin ($p = 0.019$) and center or invasive margin ($p = 0.038$). The results of the multivariate survival analysis are summarized in Table 9 and confirmed that LAG3 expression is an independent favorable prognostic factor for OS (invasive margin, $p = 0.026$; center or invasive margin, $p = 0.026$).

3.5. Correlation of ICR expression with immune cell density and molecular classification

PD−1 expression was positively correlated with LAG3 ($\gamma = 0.631$) and TIM3 ($\gamma = 0.625$) expression (Table 10), and these were classified as strong correlations [46]. LAG3 expression was moderately correlated with TIM3 expression ($\gamma = 0.534$). In addition, the expression of these three ICRs showed significant positive correlations with the density of various immune cell types, including CD3+, CD4+, CD8+, CD68+, and CD163+ TIICs. Table 11 shows the relationship between ICR expression and the molecular classification of GC. PD−1+, LAG3+, and TIM3+ rates were significantly higher in EBV+ and MSI−H GCs than in EMT−type, p53+, and p53− GCs ($p < 0.001$). In particular, EMT−type GCs showed the lowest positive rate of ICR expression, and the TIM3+ rate was the highest among the three markers.

3.6. Combined expression status of the three ICRs by mIHC

Since the expression of PD−1, TIM3, and LAG3 was positively

Figure 7. Kaplan-Meier survival curves showing the prognostic value of Programmed cell death-1 (PD-1), T-cell immunoglobulin and mucin domain-3 (TIM-3), Lymphocyte activation gene-3 (LAG-3) expression in gastric cancer. The difference was only statistically significant in cases where LAG3 was expressed in the invasive margin (p = 0.019) and center or invasive margin (p = 0.038).

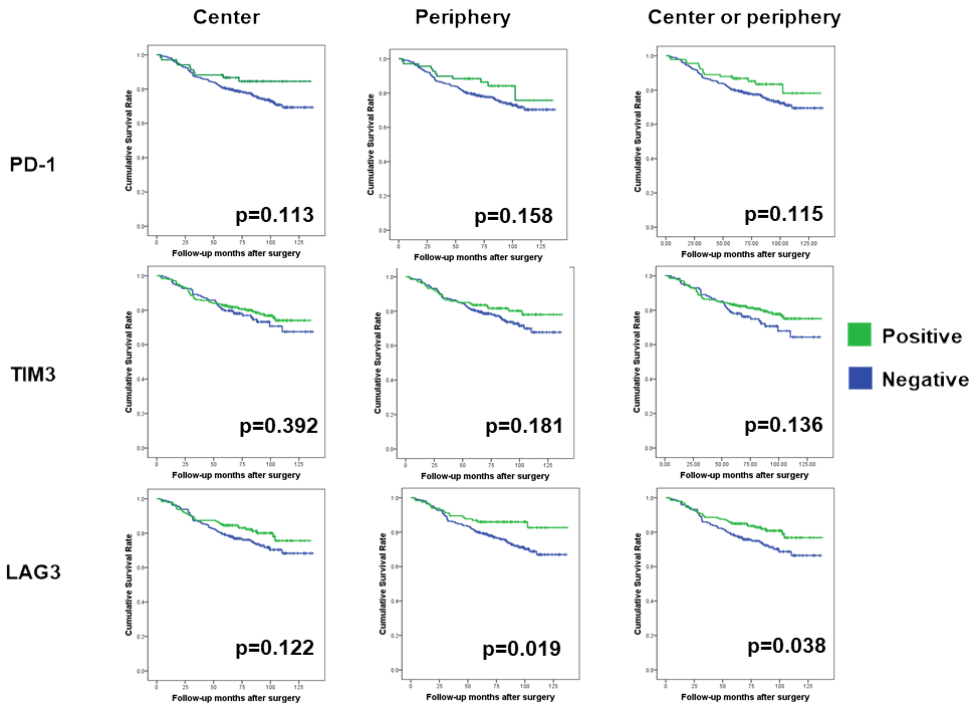

Table 9. Univariate and multivariable survival analysis by using Cox-regression analysis for immune checkpoint receptors

Variables	Univariate analysis			Multivariate analysis (LAG3 periphery)			Multivariate analysis (LAG3 center or periphery)		
	HR	95% CI	p value	HR	95% CI	p value	HR	95% CI	p value
Age	1.028	1.010 - 1.047	0.002	1.024	1.006 - 1.042	< 0.010	1.022	1.004 - 1.040	0.018
Size	1.131	1.071 - 1.193	< 0.001	1.096	1.031 - 1.165	0.003	1.094	1.028 - 1.164	0.005
Lauren classification (others vs. intestinal*)	1.443	0.914 - 2.276	0.115		-			-	
Ming classification (expanding vs. infiltrative*)	0.65	0.346 - 1.222	0.181		-			-	
Lymphatic invasion (present vs. absent*)	1.373	0.849 - 2.221	0.197		-			-	
Vascular invasion (present vs. absent*)	3.263	2.102 - 5.065	< 0.001	2.105	1.326 - 3.341	0.002	2.168	1.363 - 3.448	0.001
Perineural invasion (present vs. absent*)	2.891	1.634 - 5.114	< 0.001	1.746	0.948 - 3.215	0.074	1.824	0.992 - 3.354	0.053
pTNM (III vs. II*)	3.439	2.091 - 5.655	< 0.001	2.165	1.260 - 3.720	0.005	2.2	1.280 - 3.782	0.004
LAG3 periphery (positive vs. negative*)	0.536	0.316 - 0.908	0.020	0.540	0.315 - 0.928	0.026		-	
LAG3 center or periphery (positive vs. negative*)	0.643	0.421 - 0.980	0.040		-		0.614	0.400 - 0.944	0.026

* Reference variable;
LAG-3, Lymphocyte activation gene-3

Table 10. Correlation coefficient between immune checkpoint receptors and immune cell density

Center				Periphery			
	PD-1	LAG3	TIM3		PD-1	LAG3	TIM3
PD-1	1			PD-1	1		
LAG3	.631**	1		LAG3	.590**	1	
TIM3	.534**	.625**	1	TIM3	.422**	.592**	1
PD-L1 (CPS)	.345**	.345**	.443**	PD-L1 (CPS)	.412**	.643**	.630**
PD-L1 (TPS)	.290**	.307**	.385**	PD-L1 (TPS)	.361**	.604**	.559**
PD-L1 (ICP)	.264**	.187**	.262**	PD-L1 (ICP)	.419**	.519**	.560**
CD3	.561**	.423**	.551**	CD3	.503**	.356**	.568**
CD4	.265**	.203**	.207**	CD4	.311**	.177**	.307**
CD8	.551**	.351**	.582**	CD8	.479**	.346**	.580**
CD68	.332**	.405**	.292**	CD68	.400**	.379**	.470**
CD163	.439**	.305**	.331**	CD163	.573**	.565**	.706**
Foxp3	.342**	.219**	.276**	Foxp3	.515**	.340**	.491**

** p value < 0.01; PD-1, Programmed cell death-1; CK, Cytokeratin; TIM-3, T-cell immunoglobulin and mucin domain-3; LAG-3, Lymphocyte activation gene-3, CPS, Combined positive score; TPS. Tumor proportion score; ICP, Immune cells present

Table 11. Correlation between immune checkpoint receptors and molecular classification

Molecular classification	Total	PD-1			LAG-3			TIM-3		
		N	P	p value	N	P	p value	N	P	p value
EBV-P	25 (6.5%)	6 (2.0%)	19 (20.9%)	< 0.001	1 (0.5%)	24 (12.4%)	< 0.001	1 (0.8%)	24 (9.3%)	< 0.001
MSI-H	36 (9.4%)	16 (5.4%)	20 (22.0%)		7 (3.6%)	29 (15.0%)		4 (3.1%)	32 (12.5%)	
EMT	104 (27.0%)	100 (34.0%)	4 (4.4%)		74 (38.5%)	30 (15.5%)		47 (36.7%)	57 (22.2%)	
p53 IHC-P	70 (18.2%)	54 (18.4%)	16 (17.6%)		29 (15.1%)	41 (21.2%)		26 (20.3%)	44 (17.1%)	
p53 IHC-N	150 (39.0%)	118 (40.1%)	32 (35.2%)		81 (42.2%)	69 (35.8%)		50 (39.1%)	100 (38.9%)	
total	385	294 (76.4%)	91 (23.6%)		192 (49.9%)	193 (50.1%)		128 (33.2%)	257 (66.8%)	

N, negative; P, positive; MSI-H, microsatellite instability-high; EMT, epithelial-mesenchymal transition; IHC, immunohistochemistry

correlated, I performed chromogenic mIHC in 58 stage II and III GC cases to investigate their dual and triple expression. The density of cells with single PD−1 (red), TIM3 (green), and LAG3 (blue) expression was determined in each case (Fig. 8). Then, the density of cells with dual and triple expression was evaluated.

The mean percentage of cells with dual or triple ICR expression was 23.7% among PD−1+ cells, 26.4% among TIM3+ cells, and 32.1% among LAG3+ cells (Fig. 9a−c). The proportion of cells with single, dual, and triple expression among PD−1+, TIM3+, and LAG3+ cells varied in each case (Fig. 9d−f).

When the GC cases were classified into high and low groups based on the median PD−1+ and TIM3+ cell densities, the frequency of dual or triple expressing cells was significantly higher in the high−density group (PD−1, 30.6 ± 23.2%; TIM3, 33.8 ± 20.8%) than in the low−density group (PD−1, 16.8 ± 11.1%; TIM3, 19.1 ± 16.1%) (PD−1, $p = 0.023$; TIM3, $p < 0.001$; Fig. 9g and 9h). There was no significant difference in dual or triple expression frequency among LAG3+ cells ($p = 0.130$; Fig. 9i).

3.7. Comprehensive ICR expression analysis based on immune cell context

ICRs were mainly expressed in CD3+/CD8+ and CD3+/CD8− T cells, and minorly expressed in CD3+/Foxp3+ T cells and CD68+ macrophages (Fig. 10a). PD−1 expression was significantly higher in CD3+/CD8+ and CD3+/CD8− T cells than in CD3+/Foxp3+ T cells and CD68+ macrophages, but TIM3 expression did not significantly differ in CD68+ macrophages when compared with that in CD3+/CD8+ and CD3+/CD8− T cells (Kruskal–Wallis, PD−1, $p < 0.001$; TIM3, $p = 0.010$; Fig. 10b). LAG3 expression was significantly higher in CD3+/CD8+ T cells than in CD68+ macrophages but did not significantly differ when compared with that in CD3+/CD8− and CD3+/Foxp3+ T cells (Kruskal–Wallis, LAG3, $p = 0.008$; Fig. 10b). When comparing ICR expression by each immune cell type, PD−1 expression was the highest in

Figure 8. Single or multiple expression of markers was confirmed through multiple immunohistochemistry for each case

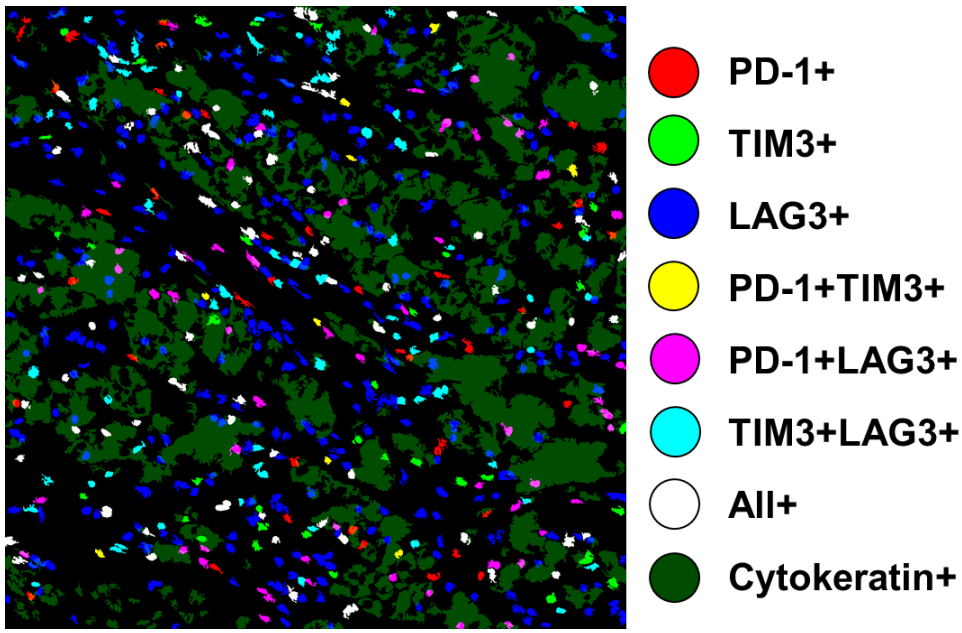

Figure 9. Combined expression of immune checkpoint receptors. Mean percentage of cells expressing single or multiple immune checkpoint receptors (ICRs): programmed death receptor 1 (PD-1) (a), T cell immunoglobulin and mucin domain 3 (TIM3) (b), and lymphocyte activation gene-3 (LAG3) (c). The proportion of cells with single, dual, and triple ICR expression varied in each case: PD-1 (d), TIM3 (e), and LAG3 (f). The frequency of double or triple ICR expression when the samples were divided into high/low density groups based on the median: PD-1 (g), TIM3 (h), and LAG3 (i).

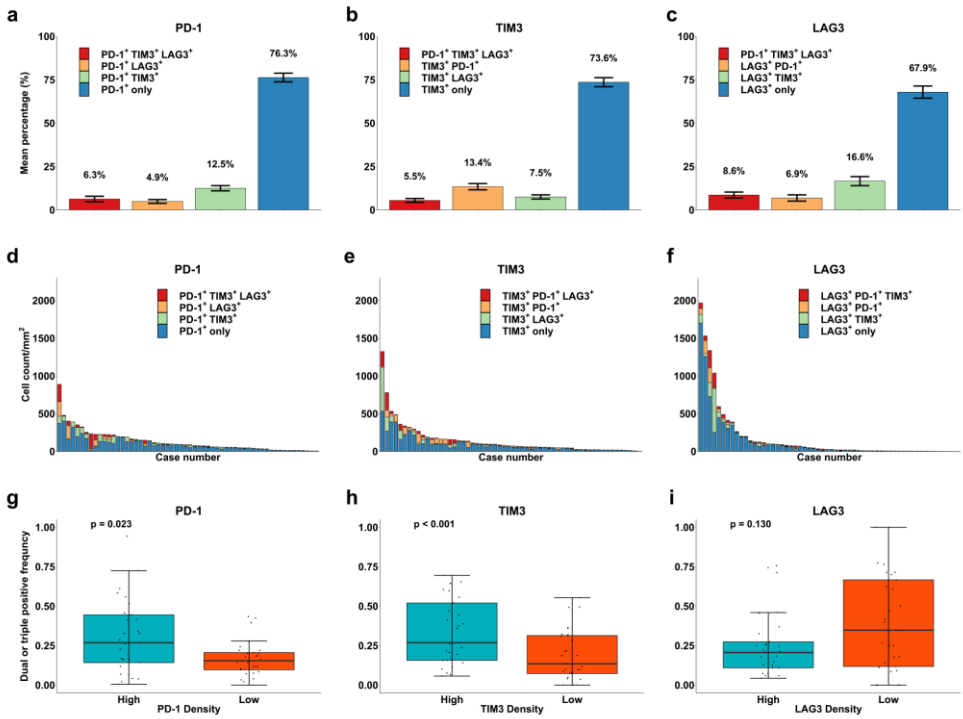

Figure 10. Immune checkpoint receptor expression based on immune context. Mean percentage of immune cell types expressing each immune checkpoint receptor (ICR): programmed death receptor 1 (PD-1), T cell immunoglobulin and mucin domain 3 (TIM3), and lymphocyte activation gene-3 (LAG3) (a). Comparison of the density of each immune cell type expressing each ICR (b). Comparison of the density of ICRs expressed by each immune cell type (c).

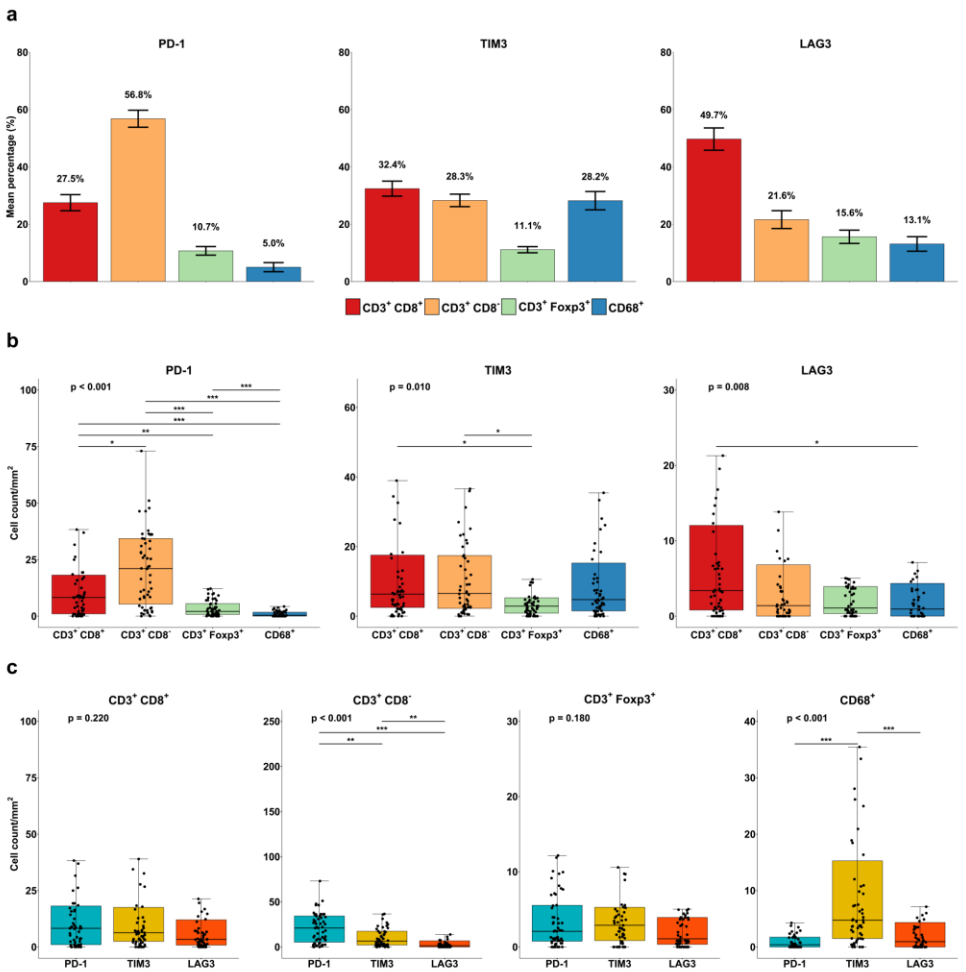

CD3+/CD8− T cells, while TIM3 expression was the highest in $CD68^+$ macrophages (Kruskal–Wallis, all $p < 0.001$, Fig. 10c). There were no significant differences in expression among the three ICRs in $CD3^+/CD8^+$ and $CD3^+/Foxp3^+$ T cells (Kruskal–Wallis, all $p > 0.05$, Fig. 10c).

In the remaining immune cells, except $CD3^+/CD8^-$ T cells, the mean proportion of double− or triple−expressing immune cells including TIM3 was higher than that without TIM3 expression. (Fig. 11a). The cell density in the presence of the expression of two or more ICRs was higher in $CD3^+/CD8^+$ T cells than in $CD68^+$ macrophages (Kruskal–Wallis, all $p < 0.001$, Fig. 11b).

Regarding the distribution between the intratumoral and stromal areas, only $CD3^+/Foxp3^+$ T cells were more distributed in the intratumoral area than in the stromal area regardless of any ICRs expression ($p < 0.001$, Fig. 12a). $CD3^+/CD8^+$ and $CD3^+/Foxp3^+$ T cells expressing any of the three ICRs were significantly more distributed in the intratumoral area than in the stromal area ($CD3^+/CD8^+/PD-1^+$, $p < 0.05$; $CD3^+/CD8^+/LAG3^+$, $p < 0.001$; $CD3^+/CD8^+$ and $CD3^+/FoxP3^+$ T cells expressing any ICRs, all $p < 0.01$, Fig. 12b).

3.8. Prognostic analysis of TIIC context and ICR expression by mIHC

The results of univariate Cox analysis showed that a positive expression of PD−1 and TIM3 was significantly positively associated with better OS (both $p < 0.01$, Fig. 13a) and PFS (both $p < 0.001$, Fig. 13b), unlike in the single IHC. A positive expression of LAG3 was statistically significant only for better PFS ($p = 0.006$; Fig. 13b). High numbers of $CD3^+/CD8^+$ and $CD3^+/CD8^-$ T cells among TIICs were associated with better OS (all $p < 0.05$, Fig. 13a) and PFS (all $p < 0.01$, Fig. 13b). When not considering ICR expression, high CD3+/Foxp3+ T cells showed no statistical significance in either better OS ($p = 0.269$, Fig. 13a) or PFS ($p = 0.085$, Fig. 13b), but high CD3+/Foxp3+ cells with TIM3

Figure 11. The mean proportion of single, dual and triple immune checkpoint receptors (ICRs) expression by immune cell type (a). The cell density by immune cell type in the presence of the expression of two or more ICRs (b)

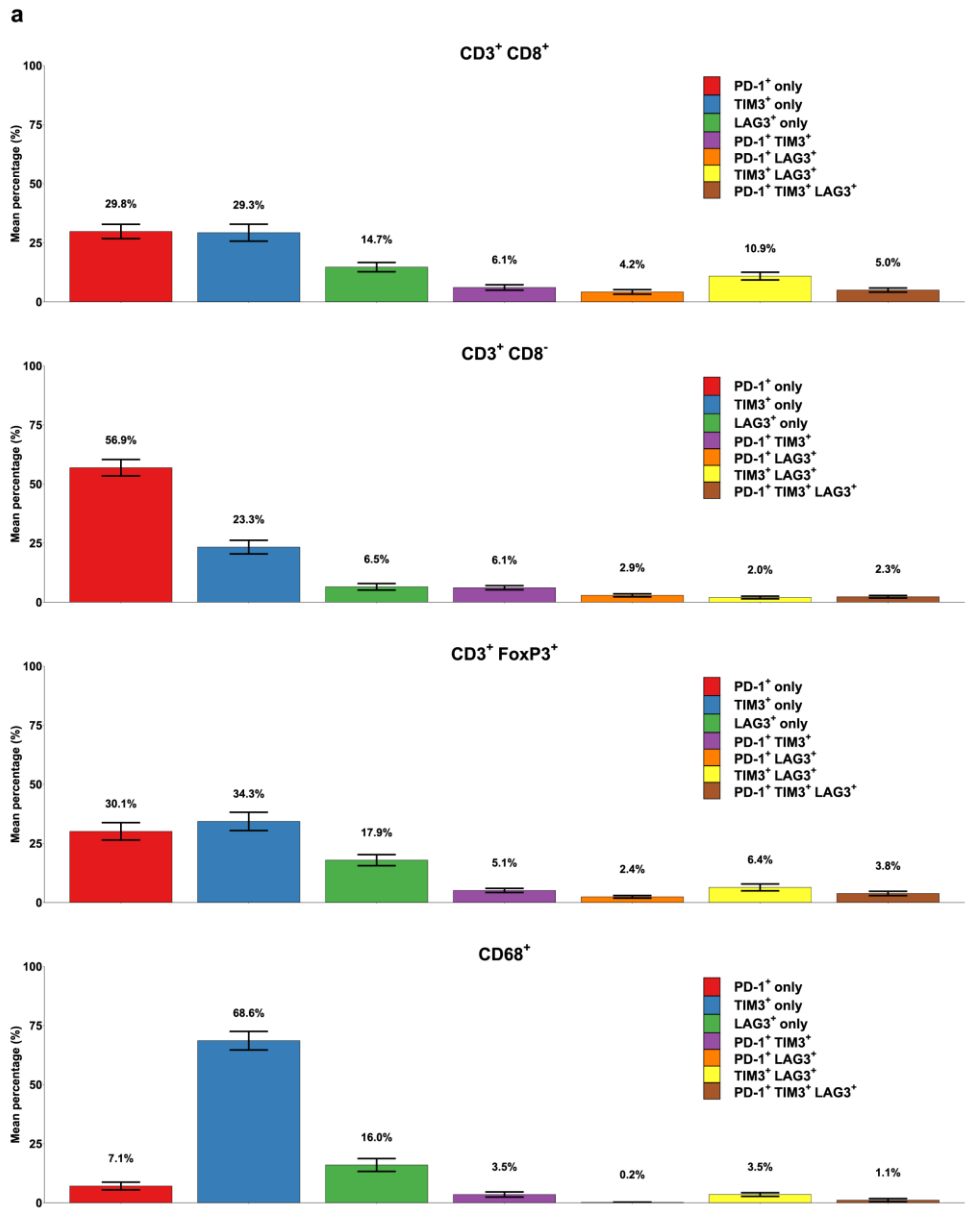

b

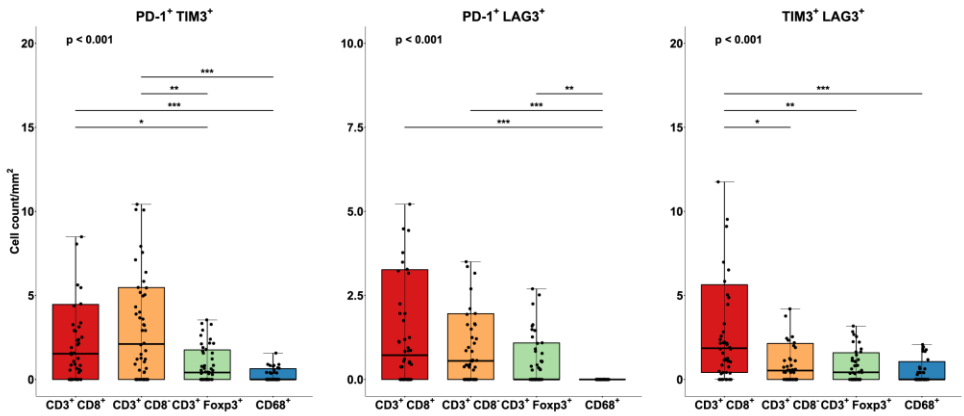
PD-1+ TIM3+
p < 0.001
PD-1+ LAG3+
p < 0.001
TIM3+ LAG3+
p < 0.001
Cell count/mm2
CD3+ CD8+
CD3+ CD8- CD3+ Foxp3+
CD68+

Figure 12. Differences in immune checkpoint receptor expression between tumors and stroma. Comparison of immune cell types between tumor and stromal areas (a). Comparison of immune cell types expressing immune checkpoint receptors between tumor and stromal areas (b).

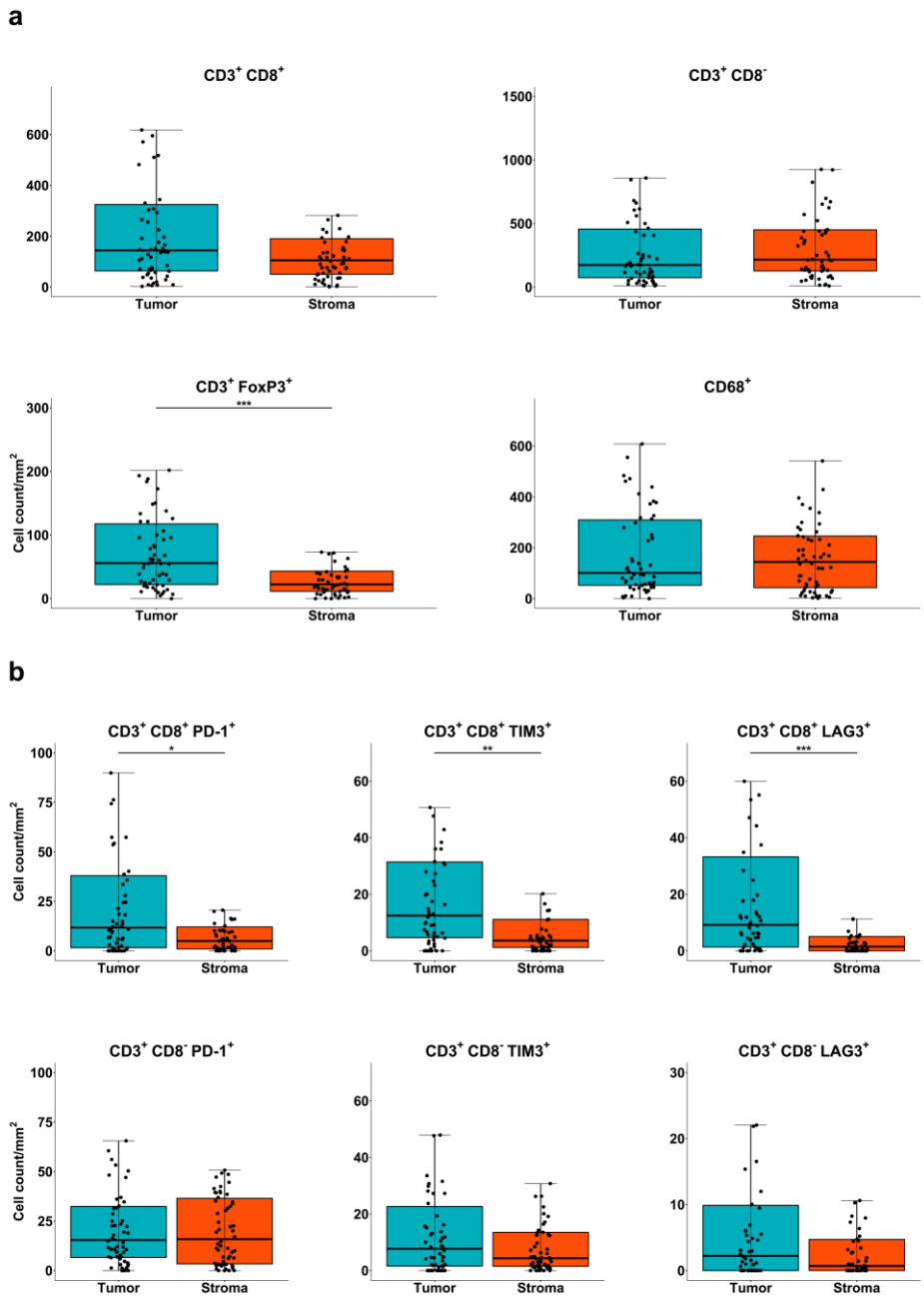

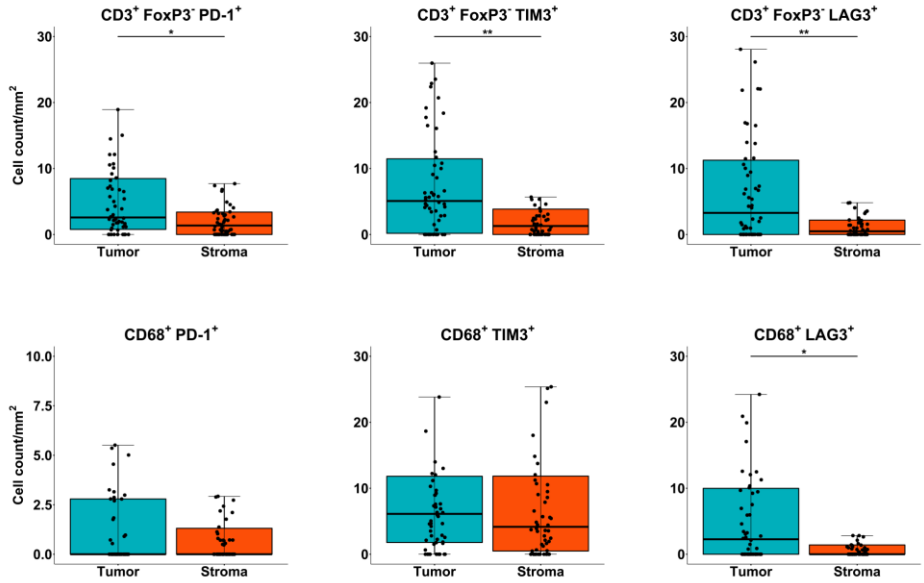
CD3+ FoxP3- PD-1+
CD3+ FoxP3- TIM3+
CD3+ FoxP3- LAG3+
CD68+ PD-1+
CD68+ TIM3+
CD68+ LAG3+
Cell count/mm2
Tumor
Stroma
*
**

Figure 13. Forest plot for univariable Cox analysis. Each tumor infiltrating immune cell (TIIC) type and immune checkpoint receptors (ICRs), overall survival (OS) (a) and progression-frees survival (PFS) (b). Analysis results for each type of TIIC expressing the ICRs, OS (c) and PFS(d).

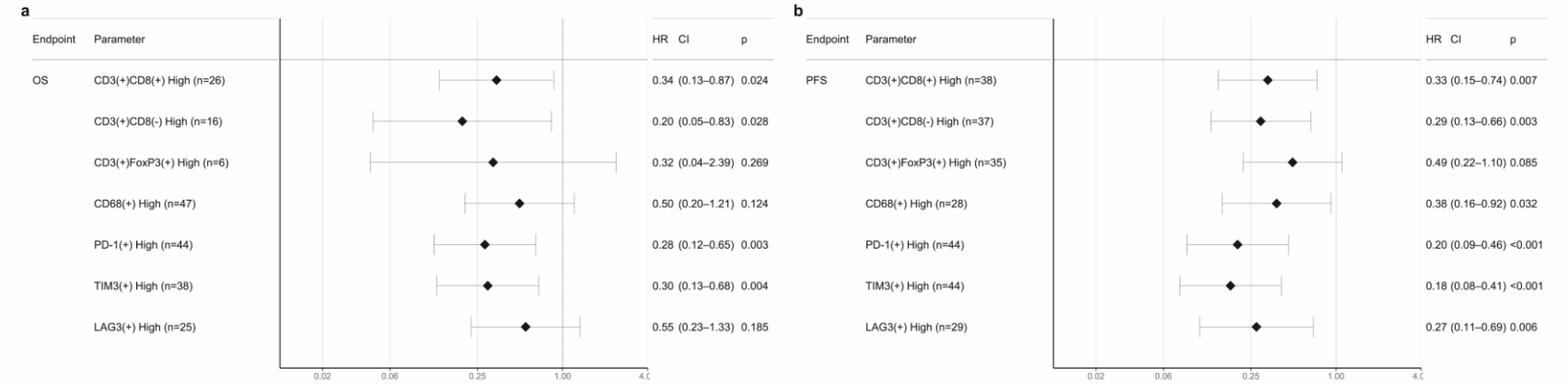

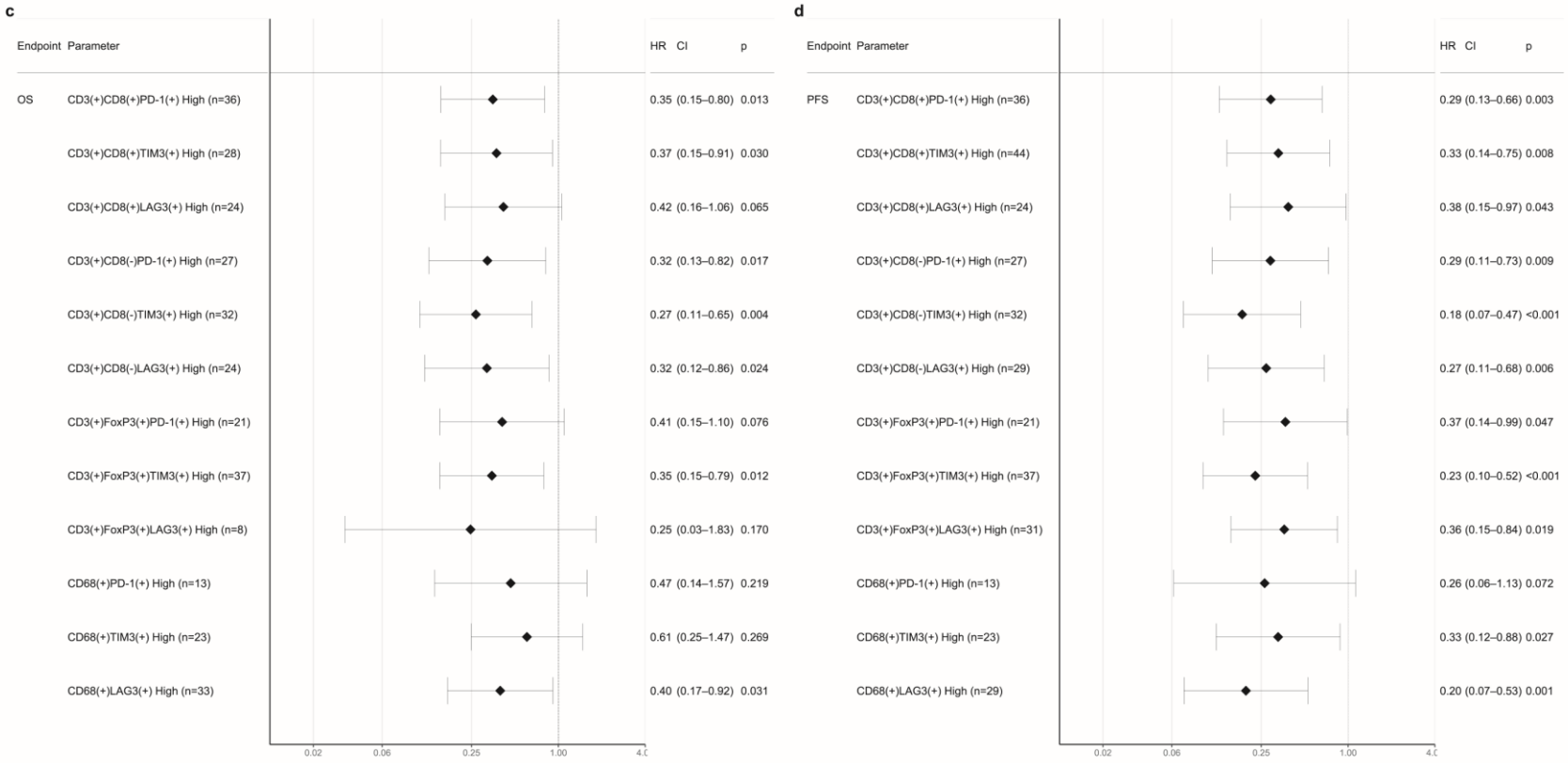
c
Endpoint Parameter
HR CI p
OS CD3(+)CD8(+)PD-1(+) High (n=36) 0.35 (0.15–0.80) 0.013
CD3(+)CD8(+)TIM3(+) High (n=28) 0.37 (0.15–0.91) 0.030
CD3(+)CD8(+)LAG3(+) High (n=24) 0.42 (0.16–1.06) 0.065
CD3(+)CD8(-)PD-1(+) High (n=27) 0.32 (0.13–0.82) 0.017
CD3(+)CD8(-)TIM3(+) High (n=32) 0.27 (0.11–0.65) 0.004
CD3(+)CD8(-)LAG3(+) High (n=24) 0.32 (0.12–0.86) 0.024
CD3(+)FoxP3(+)PD-1(+) High (n=21) 0.41 (0.15–1.10) 0.076
CD3(+)FoxP3(+)TIM3(+) High (n=37) 0.35 (0.15–0.79) 0.012
CD3(+)FoxP3(+)LAG3(+) High (n=8) 0.25 (0.03–1.83) 0.170
CD68(+)PD-1(+) High (n=13) 0.47 (0.14–1.57) 0.219
CD68(+)TIM3(+) High (n=23) 0.61 (0.25–1.47) 0.269
CD68(+)LAG3(+) High (n=33) 0.40 (0.17–0.92) 0.031
0.02
0.06
0.25
1.00
d
Endpoint Parameter
HR CI p
PFS CD3(+)CD8(+)PD-1(+) High (n=36) 0.29 (0.13–0.66) 0.003
CD3(+)CD8(+)TIM3(+) High (n=44) 0.33 (0.14–0.75) 0.008
CD3(+)CD8(+)LAG3(+) High (n=24) 0.38 (0.15–0.97) 0.043
CD3(+)CD8(-)PD-1(+) High (n=27) 0.29 (0.11–0.73) 0.009
CD3(+)CD8(-)TIM3(+) High (n=32) 0.18 (0.07–0.47) <0.001
CD3(+)CD8(-)LAG3(+) High (n=29) 0.27 (0.11–0.68) 0.006
CD3(+)FoxP3(+)PD-1(+) High (n=21) 0.37 (0.14–0.99) 0.047
CD3(+)FoxP3(+)TIM3(+) High (n=37) 0.23 (0.10–0.52) <0.001
CD3(+)FoxP3(+)LAG3(+) High (n=31) 0.36 (0.15–0.84) 0.019
CD68(+)PD-1(+) High (n=13) 0.26 (0.06–1.13) 0.072
CD68(+)TIM3(+) High (n=23) 0.33 (0.12–0.88) 0.027
CD68(+)LAG3(+) High (n=29) 0.20 (0.07–0.53) 0.001
0.02
0.06
0.25
1.00

expression showed statistically significant improvements in OS ($p = 0.012$, Fig. 13c) and PFS ($p < 0.001$, Fig. 13d).

PD-1+/TIM3+ and TIM3+/LAG3+ dual expression showed better OS ($p < 0.05$, Fig. 14a) and PFS ($p < 0.001$, Fig. 14b), but PD-1+/LAG3+ showed better results only for PFS ($p = 0.043$, Fig. 14b).

3.9. Cluster analysis of TIIC context with ICR expression

Using the TIIC context associated with the expression of the three ICRs, three clusters were identified by unsupervised hierarchical cluster analysis (Fig. 15a). The three clusters could be divided into high, medium, and low clusters according to the degree of immune cell density. Most EBV molecular types were located in the high cluster, but the MSI, EMT, p53+, and p53- types did not differ by cluster. The difference in OS among the three groups was not statistically significant ($p = 0.38$, Fig. 15b), but regarding PFS, the clusters with many ICR-expressing immune cells showed significantly better prognosis ($p = 0.014$, Fig. 15c).

Figure 14. Forest plot for univariable Cox analysis in dual expression of immune checkpoint receptors, overall survival (OS) (a) and progression-frees survival (PFS) (b).

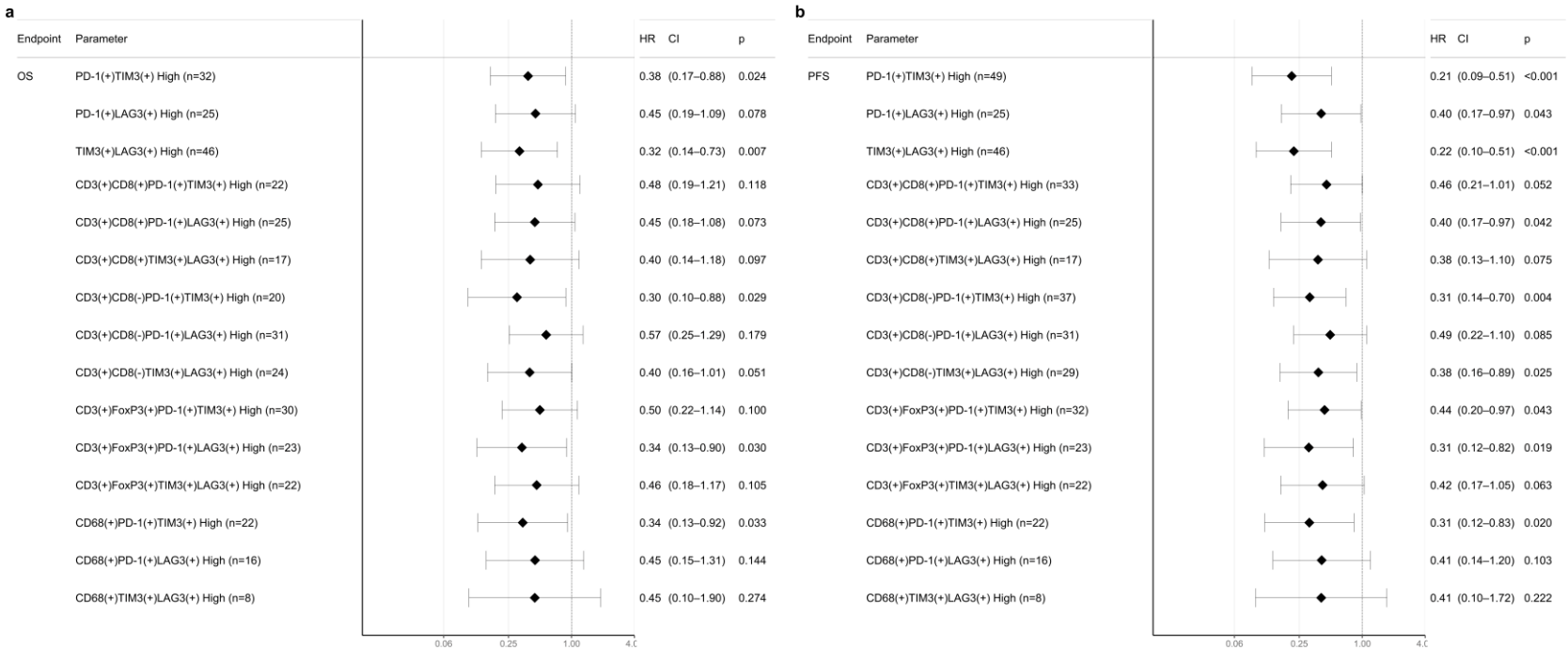

Figure 15. Association between tumor infiltrating immune cell (TIIC) context and the expression of three immune checkpoint receptors (ICRs). Three cluster were identified by unsupervised hierarchical cluster analysis (a). Kaplan Meier survival analysis of the overall survival (OS) (b) and progression-free survival (PFS) (c) in each cluster.

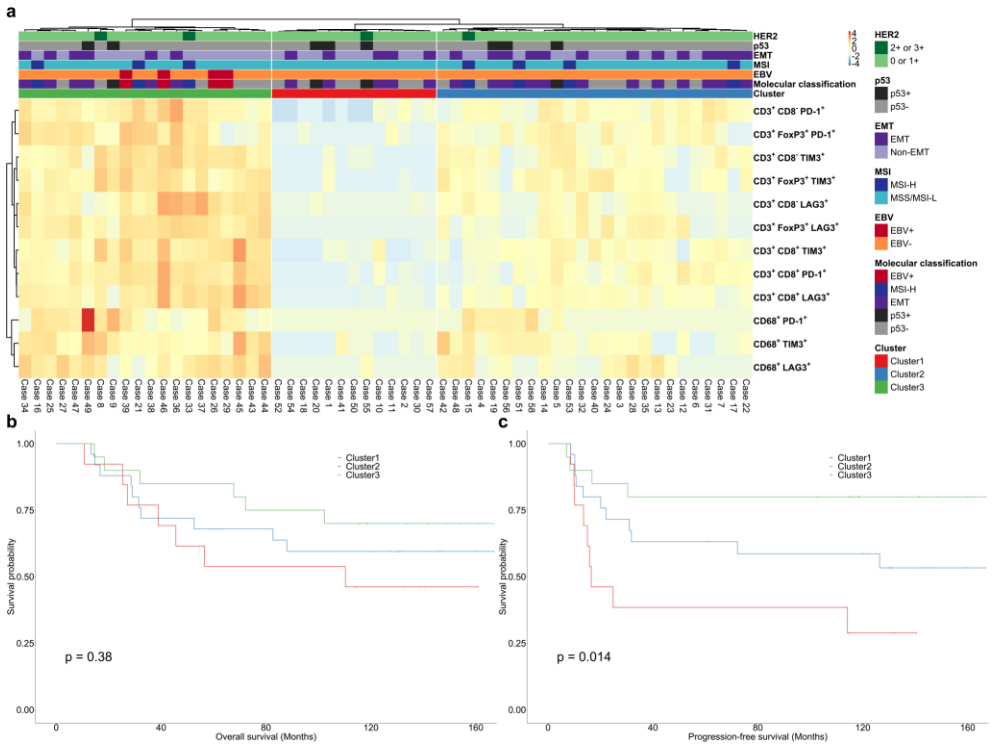

Chapter 4. Discussion

4.1. Expression loss of HLA class I in stage II and III gastric cancer

HLA I molecules are critical mediators of cytotoxic T-cell responses. HLA I molecule expression is downregulated or lost in various carcinomas and is considered as an immune escape mechanism of tumor cells [47, 48]. The mechanisms of HLA I downregulation or loss include mutation, deletion, or loss of heterozygosity in β2M and HLA I heavy chain genes, inhibition of transcription or translation of HLA antigen heavy chain, defects in HLA antigen processing regulatory mechanisms, and defects in antigen processing machinery components [49]. HLA I molecule abnormalities are classified into total HLA I antigen loss, HLA I downregulation, and selective loss or downregulation of HLA I allospecificities [49]. In recent studies, HLA I downregulation or loss in GC was reported to vary from approximately 19% to 75%. This may be due to differences in the preparation of tissue sections, primary antibodies, and scoring systems used [39, 50-52]. In previous studies, HLA I expression by IHC was interpreted as positive when the membrane of tumor cells was stained [39, 50-52]. The same method was used in this study.

Although downregulation or loss of HLA I expression has been reported in various type of cancers, including GC, HLA I expression patterns were complex in gastric cancer and autologous gastric mucosa. Previous studies have shown that autologous mucosa lacked the expression of HLA I and HLA II antigens before becoming malignant. In addition, GC showed higher expression of HLA I antigen than autologous mucosa [53]. Similar to previous studies, I observed that autologous mucosa tissues showed loss of HLA A/B/C expression predominantly in frozen sections, and significantly lower expression in FFPE sections. In one case, HLA A/B/C expression in the tumor tissue was different between the FFPE sections and the frozen sections, which may be due to

intratumoral heterogeneity observed in the previous studies as well [53].

Since HLA I molecules play an important role in restricting carcinoma-specific antigen recognition by $CD8^+$ cytotoxic T cells, the loss of HLA I is the most important escape pathway from $CD8^+$ cytotoxic T cell surveillance [48]. Additionally, loss or downregulation of HLA I expression was reported to be associated with poor prognosis in various carcinomas including non-small cell lung cancer [54], endometrial cancer [55], colorectal cancer [56], primary laryngeal squamous cell carcinoma [57], biliary tract cancer [58], and bladder cancer [59]. In contrast, the patients with downregulated HLA I expression were reported to have good prognosis in some studies, including colorectal cancer [60] and breast cancer [61]. In a study of GC, two conflicting prognostic outcomes for HLA I loss have been reported [39, 50-52]. In this study, HLA I expression loss was found to be an independent poor prognostic factor by univariate and multivariate survival analyses. Previous studies were performed in a heterogeneous GC population [39, 50-52], whereas this study was performed in a relatively homogeneous cohort of patients with stage II and III GC who were treated with fluoropyrimidine-based adjuvant chemotherapy after curative surgical resection. In addition, this study revealed the clinicopathologic importance of the expression loss of HLA I molecules in the largest GC cohort to date. Therefore, I cautiously suggest that the results of survival analysis in this study are relatively more reliable compared to those of the previous studies on heterogeneous populations.

HLA I not only mediates the $CD8^+$ cytotoxic T cell response but also inhibits NK cells by binding to inhibitory receptors. Therefore, HLA I loss could lead to escape from $CD8^+$ cytotoxic T cell response but may activate a cytotoxic NK cell response. Cancer cells are believed to regulate the level of HLA I expression in order to establish a balance between inhibiting NK cell cytotoxicity and escaping from $CD8^+$ cytotoxic T cells. The situation of cancer cells under the pressure to maintain this balance could be reflected in the

heterogeneous loss of HLA I [48]. Heterogenous loss of HLA I expression has been shown to correlate with clinicopathologic features including stages or grades and either good or poor prognosis in previous studies [50–52, 55, 56, 58, 60, 62, 63]. In this study, heterologous expression of HLA I was associated with histologic grades and was considered to affect good prognosis. These results suggest that heterogeneous expression of HLA–I may more potently inhibit $CD8^+$ cytotoxic T cell response than activated NK cells. Further studies on HLA I expression and the relationship between $CD8^+$ cytotoxic T cells, NK cells, and tumor cells are needed.

Recent studies on the relationship between PD–L1 expression and HLA I expression in lung cancer have been unable to establish a significant correlation, but the loss of HLA I expression was associated with high–grade primary tumor size in PD–L1 + lung cancer [64]. In this study, intact HLA I expression was significantly correlated with positive PD–L1 expression. It might be because this study enrolled a larger cohort of patients with stage II and III GC and the HLA I and PD–L1 interpretation was also different from that of the previous studies. Therefore, further studies are needed to confirm the relationship between HLA I expression and PD–L1 expression.

In the case of PD–1 expression, similar to PD–L1 expression, studies have reported that there is no significant association with HLA I expression [65], but there have been reports that LAG3 expression in lymphoma [66] and TIM3 expression in breast cancer [67] have a significant association with HLA I expression. In particular, LAG3 has a positive correlation with HLA I, and these results reflect an active immune response in the tumor area [66]. This study showed a significant positive correlation with three ICRs expression and HLA I molecules. However, 42.9% in PD–1+, 64.8% in TIM3+, and 57.5% in LAG3 have lost HLA I molecular expression. This should be noted as it can contribute to the resistance mechanism of immune checkpoint inhibitors.

The previous studies have demonstrated that EBV+ and MSI-H GCs are two distinct and important subtypes according to molecular and clinicopathologic characteristics, especially tumor immune microenvironment [68]. In this study, an association was observed between HLA-I expression and EBV infection, but no association with MSI was observed. There is no previous report on the association between HLA-I and EBV infection and MSI. However, recent studies have shown that the immune signature of MSI-H GCs was inconsistent high in most cases, whereas the immune signature of EBV+ GCs was consistently high in all cases [69]. Unlike EBV+ GCs, the immune signature of MSI-H GCs was heterogeneous. Since HLA-I expression was highly correlated with T cell response, MSI-H GCs showing heterogeneity in immune signature had no significant association with HLA-I expression as observed in EBV+ GCs. According to a previous study, overexpression of wild-type p53 was associated with increased HLA-I expression [70], but I did not find a significant correlation with HLA expression due to the limitations of IHC in detecting p53 overexpression. Further studies are needed to investigate the relationship between these parameters and HLA-I expression.

Transition from positive to decreased or negative expression of HLA I in tumors has been reported to be directly correlated with the degree of T cell infiltration; thus, it is considered as one of the escape mechanisms from T cell response [71]. In addition, the association between the loss or downregulation of HLA I expression and a low density of TILs has been demonstrated in colorectal cancer [72] and pancreatic cancer [73], and low TIL densities have been reported to have an unfavorable prognostic impact. This study also revealed higher $CD8^+$ cytotoxic T cell density in GCs with intact HLA A/B/C and β2M expression, positive PD-L1 expression, and EBV positivity. Recent studies showed that $CD8^+$ cytotoxic T cells, among the types of TILs, were important for the function of immune checkpoint inhibitors [74], and heavy infiltration of TILs in EBV+ GCs showed a favorable response to immune checkpoint blockade

[75, 76]. HLA I expression can be considered as a new predictive biomarker for immune checkpoint inhibitor therapy. Recently, a phase III KEYNOTE-061 trial reported that Pembrolizumab did not reach the prespecified level of significance for improving OS compared to Paclitaxel as a second-line therapy for advanced/metastatic GC or gastroesophageal junction cancer with a PD-L1 CPS ≥1 [77]. In this study, HLA I molecule expression was lost in 61.6% of PD-L1+ GCs, 19.2% of EBV+ GCs, and 67.6% of MSI-H GCs. EBV+ GCs had a tendency of intact HLA I expression when compared to PD-L1+ GCs and MSI-H GCs. Therefore, in addition to PD-L1 expression status, assessment of other biomarkers such as TIL density and expression of HLA I molecules would be helpful for predicting the effects of PD-1 inhibitors.

4.2. Expression of the ICRs in the immune context of stage II and III gastric cancer

TILs including CD8+ T cells can infiltrate tumors and suppress their growth, but ICR expression establishes an immunosuppressive TME [78]. These ICRs can be simultaneously expressed, and it has been reported that when a high level of PD-1 is observed, TIM3 and LAG3 are expressed concurrently[79, 80]. It has also been reported that there may be a compensatory mechanism such as TIM3 and LAG3 upregulation in CD8+ T cells after receiving anti-PD-1/PD-L1 therapy [81]. Here, I observed that the expression of ICRs was positively correlated by single IHC and that dual or triple ICR expression occurred frequently in cases with high PD-1 and TIM3 expression by mIHC. These results suggest that a strategy targeting multiple checkpoints simultaneously, rather than a single inhibitory receptor, may be preferable.

I found that the distribution of CD3+/CD8+ T cells, CD3+/CD8- T cells, and CD68+ macrophages did not differ between intratumor and stromal areas when any ICRs expression was not considered. Interestingly, ICR-expressing CD3+/CD8+ T cells were more distributed in the intratumor area. In hepatocellular carcinoma, more CD8+ T cells expressing high levels of PD-1

were observed in the tumor area than in the peri-tumor area, and this was associated with tissue-resident memory T cells (TRMs) [82]. TRMs are located close to the tumor and are associated with enhanced cytotoxicity [83]. These TRMs express more checkpoint inhibitors than peripheral memory T cells in the lung [84] and breast [85]. In GC, the relationship between TRMs and the clustering of immunoreceptor-expressing T cells around the tumor has not been examined, and therefore, further studies are required.

In previous studies, PD-1 expression was found to be associated with EBV+ and MSI-H GC [86]. Here, it was found that not only PD-1, but also LAG3 and TIM3 were associated with the EBV+ and MSI-H groups. Interestingly, unlike PD-1 and LAG3, TIM3 was more expressed in EMT-type GC and diffuse-type GC than PD-1 and LAG3. Further, overexpression of TIM3 was shown to enhance the metastatic capacity of hepatocellular carcinoma cells by promoting EMT [87]. In a recent study, it was found that TIM3 is highly expressed in peritoneal metastatic samples of GC, and the response to chemotherapy was poor [88, 89]. The mechanism whereby TIM3 expression induces EMT in GC has not been clearly elucidated. Therefore, further research is needed to find an immunotheutic target for EMT-type GCs that do not respond well to chemotherapy.

I performed single and multiplex IHC for immune cell markers and ICRs, followed by survival analysis. As a result, a better prognosis was observed in cases in which LAG3 was expressed at the invasive margin of the tumor and in cases with higher numbers of tumor-infiltrating cells expressing PD-1 and TIM3. In addition, the expression of ICRs in CD3+/CD8+, CD3+/CD8- and CD8-/Foxp3+ T cells, and CD68+ macrophages was associated with a better prognosis. The prognostic implications of ICRs remain controversial. Recent studies have revealed that there was a difference in the association between the expression of ICR and prognosis depending on the type of cancer. In breast cancer, PD-1, TIM3, and LAG3 expression has been reported to improve survival [90-93], whereas TIM3 expression in ovarian

cancer [90, 94] and PD-1 and TIM3 expression in lung cancer [90, 95] are associated with poor prognosis. In GC, PD-1 expression has been associated with poor prognosis [96], but also with better survival [97]. A higher LAG3+CD4+/CD4+ T cell and LAG3+CD8+/CD8+ T cell expression ratio is associated with a better prognosis in advanced GC [98], whereas a higher TIM3+CD4+/ CD4+ T cell and TIM3+CD8+/CD8+ T cell expression ratio is associated with a poor prognosis [99]. PD-1, LAG3, and TIM3 are associated with exhausted immune cells and negative regulation of immune response [78]. However, in cancer types with good prognosis despite high expression of ICRs, high expression reflects an increased activated immune response [90]. LAG3 is expressed in activated CD4+/CD8+ T cells and regulatory T cells [100], and it has been reported that induction of LAG3 expression on the cell surface is the first step required for T cell activity [101]. In addition, the ability of TIM3 to induce immune response activity was recently confirmed [102]. I investigated the correlation between the expression of ICRs and the density of various immune cell types in GC. The results also confirmed a significant positive correlation between ICRs and TIICs.

Co-expression of ICRs has been associated with poor prognosis in renal cell carcinoma [103], ovarian cancer [94], and hepatocellular carcinoma [82], but no studies have been reported so far in GC. Here, by implementing mIHC technique in a large cohort of GC, I were able to assess the co-expression status of PD-1, TIM3, or LAG3, and proved a significant association toward better prognosis. As mentioned above, the effect of ICR expression on prognosis differs among cancer types. However, the research methods employed in the studies also differed, which may explain the observed differences. In addition, my cohort size used to examine co-expression by mIHC was small. Therefore, further research using a larger cohort of GCs is needed.

4.3. Limitations

Our study has some limitations that are worth mentioning. This was

a retrospective study conducted at a single institution and sampling bias might have included owing to the TMA slides used and mIHC was performed in a small cohort. The absence of interpretation and scoring guidelines for HLA A/B/C and β2M expressions was another limitation of this study. However, compared to the previous studies, However, I were able to limit confounding factors on prognostic analysis using a relatively homogeneous cohort consisting of patients with stage II and III GC who received curative surgical resection followed by fluoropyrimidine-based adjuvant chemotherapy. Therefore, further comprehensive studies and clinical trials are needed to confirm the implications of HLA A/B/C and β2M expressions as prognostic and predictive biomarkers in managing GC patients. Additionally, a consensus of interpretation and scoring guidelines is also necessary.

4.4. Conclusions

In summary, through single IHC, I identified the clinicopathologic significance of HLA I expression status through HLA A/B/C and β2M IHCs in a large homogeneous cohort of patients with stage II and III GC. Negative expression of HLA A/B/C and β2M was frequently observed in stage II and III GCs, and particularly correlated with the aggressive behavior of GC in addition to unfavorable prognosis. Moreover, I found that HLA A/B/C and β2M expressions were significantly correlated with host immune response status such as PD-L1, ICRs such as PD-1, TIM3, and LAG3 expression, $CD8^+$ T cell density as well as EBV infection. I also showed that the expression of PD-1, LAG3, and TIM3 was positively correlated, and using mIHC, I demonstrated that dual or triple expression of ICRs is more common in cases with high ICRs' expression by single IHC. ICRs were mainly expressed in CD3+/CD8+ and CD3+/CD8- T cells and were found to be more densely distributed in the intratumoral area than in the stromal area. Moreover, ICRs were found to be associated with a better prognosis, and clusters with a large number of ICR-expressing immune cells had a better prognosis.

In conclusion, this study suggests that the negative expression of HLA I molecules can serve as a poor prognostic factor for GC patients. Additionally, this study provides key information for the application of multiple immune checkpoint inhibitors that can be used in combination therapy to treat GC patients and should be further analyzed as a predictive biomarker for immunotherapy. Finally, this work contributes critical information for the application of effective immune checkpoint inhibitors against GC.

Bibliography

1. Ferlay J, Soerjomataram I, Dikshit R, Eser S, Mathers C, Rebelo M, et al. Cancer incidence and mortality worldwide: sources, methods and major patterns in GLOBOCAN 2012. Int J Cancer. 2015;136(5):E359-86.

2. Jung KW, Won YJ, Kong HJ, Lee ES, Community of Population-Based Regional Cancer R. Cancer Statistics in Korea: Incidence, Mortality, Survival, and Prevalence in 2015. Cancer Res Treat. 2018;50(2):303-16.

3. Jung KW, Won YJ, Kong HJ, Oh CM, Shin A, Lee JS. Survival of korean adult cancer patients by stage at diagnosis, 2006-2010: national cancer registry study. Cancer Res Treat. 2013;45(3):162-71.

4. Sasako M, Sakuramoto S, Katai H, Kinoshita T, Furukawa H, Yamaguchi T, et al. Five-year outcomes of a randomized phase III trial comparing adjuvant chemotherapy with S-1 versus surgery alone in stage II or III gastric cancer. J Clin Oncol. 2011;29(33):4387-93.

5. Bang YJ, Van Cutsem E, Feyereislova A, Chung HC, Shen L, Sawaki A, et al. Trastuzumab in combination with chemotherapy versus chemotherapy alone for treatment of HER2-positive advanced gastric or gastro-oesophageal junction cancer (ToGA): a phase 3, open-label, randomised controlled trial. Lancet. 2010;376(9742):687-97.

6. Fridman WH, Zitvogel L, Sautes-Fridman C, Kroemer G. The immune contexture in cancer prognosis and treatment. Nat Rev Clin Oncol. 2017;14(12):717-34.

7. Sharma P, Hu-Lieskovan S, Wargo JA, Ribas A. Primary, Adaptive, and Acquired Resistance to Cancer Immunotherapy. Cell. 2017;168(4):707-23.

8. Jhunjhunwala S, Hammer C, Delamarre L. Antigen presentation in cancer: insights into tumour immunogenicity and immune evasion. Nat Rev Cancer. 2021;21(5):298-312.

9. van der Burg SH, Arens R, Ossendorp F, van Hall T, Melief CJ. Vaccines for established cancer: overcoming the challenges posed by immune evasion. Nat Rev Cancer. 2016;16(4):219-33.
10. Cabrera T, Lara E, Romero JM, Maleno I, Real LM, Ruiz-Cabello F, et al. HLA class I expression in metastatic melanoma correlates with tumor development during autologous vaccination. Cancer Immunol Immunother. 2007;56(5):709-17.
11. Carretero R, Romero JM, Ruiz-Cabello F, Maleno I, Rodriguez F, Camacho FM, et al. Analysis of HLA class I expression in progressing and regressing metastatic melanoma lesions after immunotherapy. Immunogenetics. 2008;60(8):439-47.
12. Chen L, Han X. Anti-PD-1/PD-L1 therapy of human cancer: past, present, and future. J Clin Invest. 2015;125(9):3384-91.
13. Sharma P, Allison JP. Immune checkpoint targeting in cancer therapy: toward combination strategies with curative potential. Cell. 2015;161(2):205-14.
14. Fuchs CS, Doi T, Jang RW, Muro K, Satoh T, Machado M, et al. Safety and Efficacy of Pembrolizumab Monotherapy in Patients With Previously Treated Advanced Gastric and Gastroesophageal Junction Cancer: Phase 2 Clinical KEYNOTE-059 Trial. JAMA Oncol. 2018;4(5):e180013.
15. Fashoyin-Aje L, Donoghue M, Chen H, He K, Veeraraghavan J, Goldberg KB, et al. FDA Approval Summary: Pembrolizumab for Recurrent Locally Advanced or Metastatic Gastric or Gastroesophageal Junction Adenocarcinoma Expressing PD-L1. Oncologist. 2019;24(1):103-9.
16. Brahmer JR, Drake CG, Wollner I, Powderly JD, Picus J, Sharfman WH, et al. Phase I study of single-agent anti-programmed death-1 (MDX-1106) in refractory solid tumors: safety, clinical activity, pharmacodynamics, and immunologic correlates. J Clin Oncol. 2010;28(19):3167-75.
17. Topalian SL, Hodi FS, Brahmer JR, Gettinger SN, Smith DC, McDermott DF, et al. Safety, activity, and immune correlates of anti-PD-1 antibody in cancer. N Engl J Med. 2012;366(26):2443-

54.
18. Muro K, Chung HC, Shankaran V, Geva R, Catenacci D, Gupta S, et al. Pembrolizumab for patients with PD-L1-positive advanced gastric cancer (KEYNOTE-012): a multicentre, open-label, phase 1b trial. Lancet Oncol. 2016;17(6):717-26.
19. Taube JM, Klein A, Brahmer JR, Xu H, Pan X, Kim JH, et al. Association of PD-1, PD-1 ligands, and other features of the tumor immune microenvironment with response to anti-PD-1 therapy. Clin Cancer Res. 2014;20(19):5064-74.
20. Marabelle A, Aspeslagh S, Postel-Vinay S, Soria JC. JAK Mutations as Escape Mechanisms to Anti-PD-1 Therapy. Cancer Discov. 2017;7(2):128-30.
21. Garrido F, Cabrera T, Aptsiauri N. "Hard" and "soft" lesions underlying the HLA class I alterations in cancer cells: implications for immunotherapy. Int J Cancer. 2010;127(2):249-56.
22. del Campo AB, Kyte JA, Carretero J, Zinchencko S, Mendez R, Gonzalez-Aseguinolaza G, et al. Immune escape of cancer cells with beta2-microglobulin loss over the course of metastatic melanoma. Int J Cancer. 2014;134(1):102-13.
23. Azuma T, Yao S, Zhu G, Flies AS, Flies SJ, Chen L. B7-H1 is a ubiquitous antiapoptotic receptor on cancer cells. Blood. 2008;111(7):3635-43.
24. Koh J, Ock CY, Kim JW, Nam SK, Kwak Y, Yun S, et al. Clinicopathologic implications of immune classification by PD-L1 expression and CD8-positive tumor-infiltrating lymphocytes in stage II and III gastric cancer patients. Oncotarget. 2017;8(16):26356-67.
25. Wang JH, Meijers R, Xiong Y, Liu JH, Sakihama T, Zhang R, et al. Crystal structure of the human CD4 N-terminal two-domain fragment complexed to a class II MHC molecule. Proc Natl Acad Sci U S A. 2001;98(19):10799-804.
26. Andrews LP, Marciscano AE, Drake CG, Vignali DA. LAG3 (CD223) as a cancer immunotherapy target. Immunol Rev. 2017;276(1):80-96.
27. Pardoll DM. The blockade of immune checkpoints in cancer

immunotherapy. Nat Rev Cancer. 2012;12(4):252-64.
28. Du W, Yang M, Turner A, Xu C, Ferris RL, Huang J, et al. TIM-3 as a Target for Cancer Immunotherapy and Mechanisms of Action. Int J Mol Sci. 2017;18(3).
29. Das M, Zhu C, Kuchroo VK. Tim-3 and its role in regulating anti-tumor immunity. Immunol Rev. 2017;276(1):97-111.
30. Grossmann KF, Othus M, Tarhini AA, Patel SP, Moon J, Sondak VK, et al. SWOG S1404: A phase III randomized trial comparing standard of care adjuvant therapy to pembrolizumab in patients with high risk resected melanoma. J Clin Oncol. 2016;34(suppl):e21032.
31. Malhotra J, Jabbour SK, Aisner J. Current state of immunotherapy for non-small cell lung cancer. Transl Lung Cancer Res. 2017;6(2):196-211.
32. Li J, Ni L, Dong C. Immune checkpoint receptors in cancer: redundant by design? Curr Opin Immunol. 2017;45:37-42.
33. Woo SR, Turnis ME, Goldberg MV, Bankoti J, Selby M, Nirschl CJ, et al. Immune inhibitory molecules LAG-3 and PD-1 synergistically regulate T-cell function to promote tumoral immune escape. Cancer Res. 2012;72(4):917-27.
34. Fourcade J, Sun Z, Benallaoua M, Guillaume P, Luescher IF, Sander C, et al. Upregulation of Tim-3 and PD-1 expression is associated with tumor antigen-specific CD8+ T cell dysfunction in melanoma patients. J Exp Med. 2010;207(10):2175-86.
35. Bang YJ, Van Cutsem E, Fuchs CS, Ohtsu A, Tabernero J, Ilson DH, et al. KEYNOTE-585: Phase III study of perioperative chemotherapy with or without pembrolizumab for gastric cancer. Future Oncol. 2019;15(9):943-52.
36. Galluzzi L, Buque A, Kepp O, Zitvogel L, Kroemer G. Immunological Effects of Conventional Chemotherapy and Targeted Anticancer Agents. Cancer Cell. 2015;28(6):690-714.
37. Zitvogel L, Galluzzi L, Smyth MJ, Kroemer G. Mechanism of action of conventional and targeted anticancer therapies: reinstating immunosurveillance. Immunity. 2013;39(1):74-88.
38. Yun S, Koh J, Nam SK, Park JO, Lee SM, Lee K, et al.

Clinical significance of overexpression of NRG1 and its receptors, HER3 and HER4, in gastric cancer patients. Gastric Cancer. 2018;21(2):225-36.
39. Lee HW, Min SK, Ju YS, Sung J, Lim MS, Yang DH, et al. Prognostic significance of HLA class I expressing in gastric carcinoma defined by monoclonal anti-pan HLA class I antibody, EMR8-5. J Gastrointest Surg. 2011;15(8):1336-43.
40. Park Y, Koh J, Na HY, Kwak Y, Lee KW, Ahn SH, et al. PD-L1 Testing in Gastric Cancer by the Combined Positive Score of the 22C3 PharmDx and SP263 Assay with Clinically Relevant Cut-offs. Cancer Res Treat. 2020.
41. Chang MS, Lee JH, Kim JP, Kim HS, Lee HS, Kim CW, et al. Microsatellite instability and Epstein-Barr virus infection in gastric remnant cancers. Pathol Int. 2000;50(6):486-92.
42. Seo AN, Kwak Y, Kim DW, Kang SB, Choe G, Kim WH, et al. HER2 status in colorectal cancer: its clinical significance and the relationship between HER2 gene amplification and expression. PLoS One. 2014;9(5):e98528.
43. Koh J, Lee KW, Nam SK, Seo AN, Kim JW, Kim JW, et al. Development and Validation of an Easy-to-Implement, Practical Algorithm for the Identification of Molecular Subtypes of Gastric Cancer: Prognostic and Therapeutic Implications. Oncologist. 2019;24(12):e1321-e30.
44. Koh J, Kwak Y, Kim J, Kim WH. High-Throughput Multiplex Immunohistochemical Imaging of the Tumor and Its Microenvironment. Cancer Res Treat. 2020;52(1):98-108.
45. Bester AC, Lee JD, Chavez A, Lee YR, Nachmani D, Vora S, et al. An Integrated Genome-wide CRISPRa Approach to Functionalize lncRNAs in Drug Resistance. Cell. 2018;173(3):649-64 e20.
46. Evans JD. Straightforward Statistics for the Behavioral Sciences. Pacific Grove, CA: Brooks/Cole Publishing Company; 1996.
47. Seliger B, Cabrera T, Garrido F, Ferrone S. HLA class I antigen abnormalities and immune escape by malignant cells. Semin

Cancer Biol. 2002;12(1):3-13.
48. Du C, Wang Y. The immunoregulatory mechanisms of carcinoma for its survival and development. J Exp Clin Cancer Res. 2011;30:12.
49. Seliger B. Novel insights into the molecular mechanisms of HLA class I abnormalities. Cancer Immunol Immunother. 2012;61(2):249-54.
50. Ueda Y, Ishikawa K, Shiraishi N, Yokoyama S, Kitano S. Clinical significance of HLA class I heavy chain expression in patients with gastric cancer. J Surg Oncol. 2008;97(5):451-5.
51. Ishigami S, Natsugoe S, Nakajo A, Arigami T, Kitazono M, Okumura H, et al. HLA-class I expression in gastric cancer. J Surg Oncol. 2008;97(7):605-8.
52. Shen YQ, Zhang JQ, Miao FQ, Zhang JM, Jiang Q, Chen H, et al. Relationship between the downregulation of HLA class I antigen and clinicopathological significance in gastric cancer. World Journal of Gastroenterology : WJG. 2005;11(23):3628-31.
53. Ferron A, Perez-Ayala M, Concha A, Cabrera T, Redondo M, Oliva MR, et al. MHC class I and II antigens on gastric carcinomas and autologous mucosa. J Immunogenet. 1989;16(4-5):413-23.
54. Hanagiri T, Shigematsu Y, Shinohara S, Takenaka M, Oka S, Chikaishi Y, et al. Clinical significance of expression of cancer/testis antigen and down-regulation of HLA class-I in patients with stage I non-small cell lung cancer. Anticancer research. 2013;33(5):2123-8.
55. Yakabe K, Murakami A, Nishimoto Y, Kajimura T, Sueoka K, Sugino N. Clinical implications of human leukocyte antigen class I expression in endometrial cancer. Mol Clin Oncol. 2015;3(6):1285-90.
56. Watson NF, Ramage JM, Madjd Z, Spendlove I, Ellis IO, Scholefield JH, et al. Immunosurveillance is active in colorectal cancer as downregulation but not complete loss of MHC class I expression correlates with a poor prognosis. Int J Cancer. 2006;118(1):6-10.
57. Ogino T, Shigyo H, Ishii H, Katayama A, Miyokawa N,

Harabuchi Y, et al. HLA class I antigen down-regulation in primary laryngeal squamous cell carcinoma lesions as a poor prognostic marker. Cancer Res. 2006;66(18):9281-9.
58. Goeppert B, Frauenschuh L, Zucknick M, Roessler S, Mehrabi A, Hafezi M, et al. Major histocompatibility complex class I expression impacts on patient survival and type and density of immune cells in biliary tract cancer. Br J Cancer. 2015;113(9):1343-9.
59. Homma I, Kitamura H, Torigoe T, Tanaka T, Sato E, Hirohashi Y, et al. Human leukocyte antigen class I down-regulation in muscle-invasive bladder cancer: its association with clinical characteristics and survival after cystectomy. Cancer Sci. 2009;100(12):2331-4.
60. Menon AG, Morreau H, Tollenaar RA, Alphenaar E, Van Puijenbroek M, Putter H, et al. Down-regulation of HLA-A expression correlates with a better prognosis in colorectal cancer patients. Lab Invest. 2002;82(12):1725-33.
61. Madjd Z, Spendlove I, Pinder SE, Ellis IO, Durrant LG. Total loss of MHC class I is an independent indicator of good prognosis in breast cancer. Int J Cancer. 2005;117(2):248-55.
62. Redondo M, Concha A, Oldiviela R, Cueto A, Gonzalez A, Garrido F, et al. Expression of HLA class I and II antigens in bronchogenic carcinomas: its relationship to cellular DNA content and clinical-pathological parameters. Cancer Res. 1991;51(18):4948-54.
63. Saio M, Teicher M, Campbell G, Feiner H, Delgado Y, Frey AB. Immunocytochemical demonstration of down regulation of HLA class-I molecule expression in human metastatic breast carcinoma. Clin Exp Metastasis. 2004;21(3):243-9.
64. Perea F, Sanchez-Palencia A, Gomez-Morales M, Bernal M, Concha A, Garcia MM, et al. HLA class I loss and PD-L1 expression in lung cancer: impact on T-cell infiltration and immune escape. Oncotarget. 2018;9(3):4120-33.
65. Cao J, Brouwer NJ, Jordanova ES, Marinkovic M, van Duinen SG, de Waard NE, et al. HLA Class I Antigen Expression in

Conjunctival Melanoma Is Not Associated With PD-L1/PD-1 Status. Invest Ophthalmol Vis Sci. 2018;59(2):1005-15.
66. Gould C, Lickiss J, Kankanige Y, Yerneni S, Lade S, Gandhi MK, et al. Characterisation of immune checkpoints in Richter syndrome identifies LAG3 as a potential therapeutic target. Br J Haematol. 2021;195(1):113-8.
67. Messaoudene M, Mourikis TP, Michels J, Fu Y, Bonvalet M, Lacroix-Trikki M, et al. T-cell bispecific antibodies in node-positive breast cancer: novel therapeutic avenue for MHC class I loss variants. Ann Oncol. 2019;30(6):934-44.
68. Cancer Genome Atlas Research N. Comprehensive molecular characterization of gastric adenocarcinoma. Nature. 2014;513(7517):202-9.
69. Kim ST, Cristescu R, Bass AJ, Kim KM, Odegaard JI, Kim K, et al. Comprehensive molecular characterization of clinical responses to PD-1 inhibition in metastatic gastric cancer. Nat Med. 2018;24(9):1449-58.
70. Wang B, Niu D, Lai L, Ren EC. p53 increases MHC class I expression by upregulating the endoplasmic reticulum aminopeptidase ERAP1. Nat Commun. 2013;4:2359.
71. Aptsiauri N, Ruiz-Cabello F, Garrido F. The transition from HLA-I positive to HLA-I negative primary tumors: the road to escape from T-cell responses. Curr Opin Immunol. 2018;51:123-32.
72. Kasajima A, Sers C, Sasano H, Johrens K, Stenzinger A, Noske A, et al. Down-regulation of the antigen processing machinery is linked to a loss of inflammatory response in colorectal cancer. Hum Pathol. 2010;41(12):1758-69.
73. Ryschich E, Notzel T, Hinz U, Autschbach F, Ferguson J, Simon I, et al. Control of T-cell-mediated immune response by HLA class I in human pancreatic carcinoma. Clin Cancer Res. 2005;11(2 Pt 1):498-504.
74. Tumeh PC, Harview CL, Yearley JH, Shintaku IP, Taylor EJ, Robert L, et al. PD-1 blockade induces responses by inhibiting adaptive immune resistance. Nature. 2014;515(7528):568-71.

75. Rooney MS, Shukla SA, Wu CJ, Getz G, Hacohen N. Molecular and genetic properties of tumors associated with local immune cytolytic activity. Cell. 2015;160(1-2):48-61.
76. Choi YY, Noh SH, Cheong JH. Molecular Dimensions of Gastric Cancer: Translational and Clinical Perspectives. J Pathol Transl Med. 2016;50(1):1-9.
77. Shitara K, Ozguroglu M, Bang YJ, Di Bartolomeo M, Mandala M, Ryu MH, et al. Pembrolizumab versus paclitaxel for previously treated, advanced gastric or gastro-oesophageal junction cancer (KEYNOTE-061): a randomised, open-label, controlled, phase 3 trial. Lancet. 2018;392(10142):123-33.
78. Anderson AC, Joller N, Kuchroo VK. Lag-3, Tim-3, and TIGIT: Co-inhibitory Receptors with Specialized Functions in Immune Regulation. Immunity. 2016;44(5):989-1004.
79. Thommen DS, Schreiner J, Müller P, Herzig P, Roller A, Belousov A, et al. Progression of Lung Cancer Is Associated with Increased Dysfunction of T Cells Defined by Coexpression of Multiple Inhibitory Receptors. Cancer Immunol Res. 2015;3(12):1344-55.
80. Thommen DS, Koelzer VH, Herzig P, Roller A, Trefny M, Dimeloe S, et al. A transcriptionally and functionally distinct PD-1(+) CD8(+) T cell pool with predictive potential in non-small-cell lung cancer treated with PD-1 blockade. Nat Med. 2018;24(7):994-1004.
81. Bialkowski L, Van der Jeught K, Bevers S, Tjok Joe P, Renmans D, Heirman C, et al. Immune checkpoint blockade combined with IL-6 and TGF-beta inhibition improves the therapeutic outcome of mRNA-based immunotherapy. Int J Cancer. 2018;143(3):686-98.
82. Ma J, Zheng B, Goswami S, Meng L, Zhang D, Cao C, et al. PD1(Hi) CD8(+) T cells correlate with exhausted signature and poor clinical outcome in hepatocellular carcinoma. J Immunother Cancer. 2019;7(1):331.
83. Mueller SN, Mackay LK. Tissue-resident memory T cells: local specialists in immune defence. Nat Rev Immunol.

2016;16(2):79-89.
84. Ganesan AP, Clarke J, Wood O, Garrido-Martin EM, Chee SJ, Mellows T, et al. Tissue-resident memory features are linked to the magnitude of cytotoxic T cell responses in human lung cancer. Nat Immunol. 2017;18(8):940-50.
85. Savas P, Virassamy B, Ye C, Salim A, Mintoff CP, Caramia F, et al. Single-cell profiling of breast cancer T cells reveals a tissue-resident memory subset associated with improved prognosis. Nat Med. 2018;24(7):986-93.
86. De Rosa S, Sahnane N, Tibiletti MG, Magnoli F, Vanoli A, Sessa F, et al. EBV(+) and MSI Gastric Cancers Harbor High PD-L1/PD-1 Expression and High CD8(+) Intratumoral Lymphocytes. Cancers (Basel). 2018;10(4).
87. Lin H, Yang B, Teng M. T-cell immunoglobulin mucin-3 as a potential inducer of the epithelial-mesenchymal transition in hepatocellular carcinoma. Oncol Lett. 2017;14(5):5899-905.
88. Wang R, Song S, Harada K, Ghazanfari Amlashi F, Badgwell B, Pizzi MP, et al. Multiplex profiling of peritoneal metastases from gastric adenocarcinoma identified novel targets and molecular subtypes that predict treatment response. Gut. 2020;69(1):18-31.
89. Huang L, Wu RL, Xu AM. Epithelial-mesenchymal transition in gastric cancer. Am J Transl Res. 2015;7(11):2141-58.
90. Tu L, Guan R, Yang H, Zhou Y, Hong W, Ma L, et al. Assessment of the expression of the immune checkpoint molecules PD-1, CTLA4, TIM-3 and LAG-3 across different cancers in relation to treatment response, tumor-infiltrating immune cells and survival. Int J Cancer. 2020;147(2):423-39.
91. Byun KD, Hwang HJ, Park KJ, Kim MC, Cho SH, Ju MH, et al. T-Cell Immunoglobulin Mucin 3 Expression on Tumor Infiltrating Lymphocytes as a Positive Prognosticator in Triple-Negative Breast Cancer. J Breast Cancer. 2018;21(4):406-14.
92. Guo L, Cao C, Goswami S, Huang X, Ma L, Guo Y, et al. Tumoral PD-1hiCD8+ T cells are partially exhausted and predict favorable outcome in triple-negative breast cancer. Clin Sci (Lond). 2020;134(7):711-26.

93. Burugu S, Gao D, Leung S, Chia SK, Nielsen TO. LAG-3+ tumor infiltrating lymphocytes in breast cancer: clinical correlates and association with PD-1/PD-L1+ tumors. Ann Oncol. 2017;28(12):2977-84.
94. Fucikova J, Rakova J, Hensler M, Kasikova L, Belicova L, Hladikova K, et al. TIM-3 Dictates Functional Orientation of the Immune Infiltrate in Ovarian Cancer. Clin Cancer Res. 2019;25(15):4820-31.
95. Zhuang X, Zhang X, Xia X, Zhang C, Liang X, Gao L, et al. Ectopic expression of TIM-3 in lung cancers: a potential independent prognostic factor for patients with NSCLC. Am J Clin Pathol. 2012;137(6):978-85.
96. Eto S, Yoshikawa K, Nishi M, Higashijima J, Tokunaga T, Nakao T, et al. Programmed cell death protein 1 expression is an independent prognostic factor in gastric cancer after curative resection. Gastric Cancer. 2016;19(2):466-71.
97. Wu Y, Cao D, Qu L, Cao X, Jia Z, Zhao T, et al. PD-1 and PD-L1 co-expression predicts favorable prognosis in gastric cancer. Oncotarget. 2017;8(38):64066-82.
98. Ohmura H, Yamaguchi K, Hanamura F, Ito M, Makiyama A, Uchino K, et al. OX40 and LAG3 are associated with better prognosis in advanced gastric cancer patients treated with anti-programmed death-1 antibody. Br J Cancer. 2020;122(10):1507-17.
99. Cheng G, Li M, Wu J, Ji M, Fang C, Shi H, et al. Expression of Tim-3 in gastric cancer tissue and its relationship with prognosis. International journal of clinical and experimental pathology. 2015;8(8):9452-7.
100. Bae J, Lee SJ, Park CG, Lee YS, Chun T. Trafficking of LAG-3 to the surface on activated T cells via its cytoplasmic domain and protein kinase C signaling. J Immunol. 2014;193(6):3101-12.
101. Long L, Zhang X, Chen F, Pan Q, Phiphatwatchara P, Zeng Y, et al. The promising immune checkpoint LAG-3: from tumor microenvironment to cancer immunotherapy. Genes Cancer.

2018;9(5-6):176-89.
102. Ocana-Guzman R, Torre-Bouscoulet L, Sada-Ovalle I. TIM-3 Regulates Distinct Functions in Macrophages. Front Immunol. 2016;7:229.
103. Granier C, Dariane C, Combe P, Verkarre V, Urien S, Badoual C, et al. Tim-3 Expression on Tumor-Infiltrating PD-1(+)CD8(+) T Cells Correlates with Poor Clinical Outcome in Renal Cell Carcinoma. Cancer Res. 2017;77(5):1075-82.

초록

고형 종양은 종양 관련 면역 반응을 유발한다 종양 세포는 종양 세포에서 제1급 인간 백혈구 항원 (HLA I)의 손실 및 종양 침윤 면역 세포에서 면역 관문 수용체 발현 증가와 같은 종양에 대한 면역 반응을 피할 수 있는 특성을 가진다. 인간 백혈구 항원 유전자에 의해 암호화된 HLA-A, -B 또는 -C 와 베타-2-마이크로글로불린을 포함한 알파(중) 사슬로 구성된 HLA I은 CD8-양성 세포독성 T 세포에 의하여 인식되는 펩타이드 항원을 표시하는 역할을 하며 모든 유핵 세포에서 막단백질로 발현한다. 프로그램된 사멸 수용체 1(PD-1), 림프구 활성화 유전자-3(LAG3), T 세포 면역글로불린 및 뮤신 도메인 3(TIM3)과 같은 면역 관문 수용체는 암세포의 면역 관용 및 회피를 매개하므로 다양한 고형암에서 전신 요법을 위하여 면역 관문 억제제를 사용하려고 노력하였다. 그러나 위암에서 HLA I 또는 면역 관문 수용체 발현에 대한 포괄적인 분석은 부족하다. 따라서, 암세포에서 HLA I 분자 발현과 위암의 종양 침투 면역 세포에서 PD-1, LAG3, TIM3 발현의 임상 병리학적 중요성을 결정하려 한다.

조직 미세배열을 이용하여 406명의 2기 및 3기 위암 환자의 종양 중심 및 침윤 경계에서 HLA A/B/C, 베타-2-마이크로글로불린, PD-1, TIM3, LAG3, PD-L1, 종양 침투 면역 세포들에 대한 면역 조직화학 염색을 수행하였다. 면역 조직화학 염색 결과 HLA I 분자는 395건, 면역 관문 수용체는 385건이 분석에 적합 하였다. Epstein-Barr 바이러스(EBV) 제자리 부합법, 현미 부수체 불안정성(MSI) 검사, E-cadherin 및 p53 면역 조직화학 염색은 위암의 분자적 분류를 위하여 수행되었다. 그리고 PD-1, TIM3, LAG3, CD8, CD3, FOXP3, CD68 및 사이토 케라틴에 대한 발색 다중 면역 조직화학 염색 검사가 전체 검체 중 58건에서 수행되었다.

395건의 2기 및 3기 위암 환자의 검체 중 암세포의 HLA A/B/C 및 베타-2-마이크로글로불린 음성 발현이 각각 258건(65.3%)

와 235건(59.5%)에서 관찰되었다. HLA I 음성 발현은 공격적인 임상 병리학적 특징과 유의한 관련을 보였다. 또한 HLA A/B/C 및 베타-2-마이크로글로불린의 음성 발현은 CD8-양성 세포독성 T 세포 침투, EBV 양성, PD-L1 양성 발현과 역 상관관계가 있었다. HLA A/B/C 및 베타-2-마이크로글로불린의 발현이 온전한 경우 PD-1, TIM3 및 LAG3 발현과 유의미한 상관관계를 보였다. HLA A/B/C 음성 발현 위암 환자는 전체 생존기간에서 나쁜 예후를 보였으며, HLA A/B/C 및 베타-2-마이크로글로불린 둘 모두 음성 발현일 때 단 변량과 다 변량 생존 분석에서 유의하게 전체 생존기간에서 나쁜 예후와 연관성을 보였다.

PD-1, LAG3, TIM3는 각각 단일 면역 조직화학 염색 검사 결과 91(23.6%), 193(50.1%), 257(66.8%) 건의 위암 검체에서 관찰되었다. 그리고 높은 종양 침투 면역 세포 밀도, EBV 양성 및 고빈도 현미 부수체 불안정성 분자 유형과 관련이 있었다. TIM3는 PD-1 및 LAG3보다 상피-중간엽 전환 유형의 위암에서 더 많이 발현되었다. 종양의 침윤 경계에서 LAG3 발현은 단 변량 및 다 변량 생존 분석에서 더 나은 예후와 유의하게 관련이 있었다. 서로 다른 면역 관문 수용체 발현은 서로 간에 상당히 연관성이 있었다.

다중 면역 조직화학 염색 검사에 의하여 이중 또는 삼중 면역 관문 수용체 발현은 저밀도 그룹보다 높은 밀도로 PD-1 및 TIM3를 발현하는 그룹에서 더 빈번하다는 것을 확인하였다. 또한, 면역 관문 수용체는 주로 CD3 양성/CD8 양성 및 CD3 양성/CD8 음성 T 세포에서 발현하였다. 면역 관문 수용체를 발현하는 CD3 양성/CD8 양성 T 세포는 기질보다 종양 주변에 더 많이 분포하였다. 58개의 위암을 대상으로 시행한 다중 면역 조직화학 염색을 바탕으로 한 군집 분석 결과 총 3개 그룹으로 분류되었다. 그 결과, 종양 침윤 면역 세포에서 면역 관문 수용체 발현이 가장 높은 그룹에서 모든 EBV 양성 위암이 포함되었으며, 무 진행 생존기간에서 현저하게 좋은 예후를 보였다.

본 연구에서, 암세포의 HLA A/B/C 및 베타-2-마이크로글로불린 음성 발현은 공격적인 임상 병리학적 특징을 갖는 2기 및 3기 위암

에서 주로 관찰되었으며, 나쁜 예후 및 숙주 면역 상태와 연관성이 있었다. 하지만, 종양 침투 면역 세포에서의 PD-1, LAG3, TIM3 발현은 서로 간에 양의 상관관계가 있으며 단일 면역 조직 화학 염색에서 관문 수용체 발현이 높은 그룹에서 면역 관문 수용체의 이중 또는 삼중 동시 발현이 더 흔하게 관찰되었다. 또한 위암에서 면역 관문 수용체 발현은 더 나은 예후와 관련이 있었다. 마지막으로, 이 연구는 위암에 대한 효과적인 면역 관문 억제제의 적용을 위한 핵심 정보를 제공할 것이다.